

Zeitschrift: Helvetica Physica Acta
Band: 45 (1972)
Heft: 3

Artikel: Thermal radiation in finite cavities
Autor: Baltes, H.P. / Kneubühl, F.K.
DOI: <https://doi.org/10.5169/seals-114394>

Nutzungsbedingungen

Die ETH-Bibliothek ist die Anbieterin der digitalisierten Zeitschriften auf E-Periodica. Sie besitzt keine Urheberrechte an den Zeitschriften und ist nicht verantwortlich für deren Inhalte. Die Rechte liegen in der Regel bei den Herausgebern beziehungsweise den externen Rechteinhabern. Das Veröffentlichen von Bildern in Print- und Online-Publikationen sowie auf Social Media-Kanälen oder Webseiten ist nur mit vorheriger Genehmigung der Rechteinhaber erlaubt. [Mehr erfahren](#)

Conditions d'utilisation

L'ETH Library est le fournisseur des revues numérisées. Elle ne détient aucun droit d'auteur sur les revues et n'est pas responsable de leur contenu. En règle générale, les droits sont détenus par les éditeurs ou les détenteurs de droits externes. La reproduction d'images dans des publications imprimées ou en ligne ainsi que sur des canaux de médias sociaux ou des sites web n'est autorisée qu'avec l'accord préalable des détenteurs des droits. [En savoir plus](#)

Terms of use

The ETH Library is the provider of the digitised journals. It does not own any copyrights to the journals and is not responsible for their content. The rights usually lie with the publishers or the external rights holders. Publishing images in print and online publications, as well as on social media channels or websites, is only permitted with the prior consent of the rights holders. [Find out more](#)

Download PDF: 03.02.2026

ETH-Bibliothek Zürich, E-Periodica, <https://www.e-periodica.ch>

Thermal Radiation in Finite Cavities

by **H. P. Baltes** and **F. K. Kneubühl**

Solid State Physics Laboratory, Swiss Federal Institute of Technology, Zurich, Switzerland

(8. IX. 71)

Abstract. The mode density $D(\nu)$ of the electromagnetic resonances of a lossless closed cavity plays a dominant role in the theory of far-infrared radiation standards, the Einstein coefficients of spontaneous and stimulated emission, and radiation corrections as e.g. the Lamb-shift. Refinements of the Planck-Weyl asymptotic density $D_0(\nu)$ for cavities of finite size are studied by computational methods involving the first 10^6 eigenvalues. Averaging over the modes for a large bandwidth $\Delta\nu$, second order corrections of the type $D/D_0 = 1 - C \nu^{-2} V^{-2/3}$ with V = volume of the cavity are obtained for a variety of cavity geometries including the parallelepiped, the circular cylinder, the sphere, the hemisphere, and cylindrical as well as spherical sectors (wedges and cones). The relation of the constant C to the edge lengths and curvatures of the cavity is investigated.

The second order corrections resulting for the Wien displacement law and for the Lamb-shift are determined. The implications for the Stefan-Boltzmann radiation law as well as for the thermodynamical properties of the radiation field are studied. A rigorous connection between the asymptotic *spectral* and *total* radiation formulae is established in terms of Abelian and Tauberian theorems.

For narrow bandwidth $\Delta\nu$, fluctuations of the mode density are much stronger than the second order average correction. The relative mean fluctuation is found to be proportional to $\nu^{-1}(\Delta\nu)^{-1}$.

A new proof for the wellknown vanishing of the average first order or surface correction term is given in terms of the scalar E - and H -type wave potentials. Surface terms appear only if the E - and H -type densities D_E and D_H are determined separately. The surface corrections of D_E and D_H are equal, but have opposite signs. The corresponding first order refinement of the temporal autocorrelation functions of the black-body radiation field is studied.

«Es ist wohl nicht überflüssig, hier zu bemerken, dass es bis jetzt noch nicht gelungen ist, eine exakte Definition eines ‚vollkommen schwarzen‘ Körpers, welche sich auf beliebig lange Wellen anwenden lässt, aufzufinden.»

Max Planck 1898 [136]

1. Introduction

A. Thermal radiation standards in the far infrared

Far-infrared and submillimeter black-body cavity radiation standards are indispensable as reference sources for

- the measurement of the spectral emissivity of solid materials [1]–[6];
- plasma diagnostics [7]–[9];

- the calibration of spectral photometers used in astrophysical and space research [10]–[18];
- absolute radiometry used in meteorology [19]–[26].

The cavity black-bodies used in these fields can be characterized by the relations

$$\lambda \approx \frac{d}{50} \quad \text{and} \quad \Delta \left(\frac{1}{\lambda} \right) \approx \frac{1}{d}, \quad (1.1)$$

where λ represents the wavelength, $\Delta(1/\lambda)$ the spectral resolution, and d the linear dimension of the cavity. $1/d$ corresponds to the approximate separation of levels between two adjacent cavity modes. The above relations indicate that the far-infrared cavity black-bodies can be approximated neither by microwave thermal noise standards nor by optical cavity black-bodies:

The *microwave thermal noise standards* fulfil the conditions

$$\lambda \approx d \quad \text{and} \quad \Delta \left(\frac{1}{\lambda} \right) \ll \frac{1}{d}. \quad (1.2)$$

If ideal impedance matching is taken for granted, the emission is described by the *Nyquist formula*

$$I(\nu_0) = k T \Delta \nu_0 \quad (1.3)$$

with the bandwidth $\Delta \nu_0$ if the emitted single mode of the frequency ν_0 . Narrow-band thermal cavity sources have been realized that yield a noise power very close to the ideal Nyquist noise [27]–[32].

Optical cavity black-bodies, on the other hand, obey the relations

$$\lambda \ll d \quad \text{and} \quad \Delta \left(\frac{1}{\lambda} \right) \gg \frac{1}{d}, \quad (1.4)$$

which are the prerequisites [33] of *Planck's radiation formula*

$$u(\nu, T) d\nu = \frac{h \nu}{e^{h\nu/kT} - 1} D_0(\nu) d\nu, \quad (1.5)$$

with the asymptotic spectral density

$$D_0(\nu) d\nu = \frac{8 \pi}{c^3} V \nu^2 d\nu, \quad (1.6)$$

of the electromagnetic modes in a lossless closed cavity of volume V . Formula (1.5) with the mode density (1.6) is strictly valid only in the limits $\nu \rightarrow \infty$ or $V \rightarrow \infty$. According to the assumptions (1.4), optical cavity black-bodies can be calculated and constructed with the aid of geometrical optics. Many theoretical studies of this kind have been performed since Wien and Lummer first computed the emissivity of a cavity standard with a small exit hole [34]. Mainly spherical, cylindrical, and cone-shaped cavities have been studied [35]–[51]. While these theories have reached a satisfactory state, the problems of non-Lambertian [54], [55] and non-isothermal [56]–[60] cavity walls have rarely been taken into account. Only a few experimental determinations of the emissivity of optical cavity black-bodies exist [61]–[64]. In the

optical [65]–[71] as well as in the near infrared [72]–[75] spectral regions, cavity standards have been constructed with more than 99% spectral emissivity over a wide spectral band. Satisfactory standards are commercially available [76], [77].

So far, no attempt has been made to apply the technique of thermal noise standards to *far-infrared black-bodies*. On the other hand, optical cavity black-bodies have been tentatively used for this purpose [78]–[82]. As their design is based on geometrical optics, serious problems arise because of the finite ratio λ/d , the size effects of the aperture, and the resonance effects due to baffles or other obstacles in the cavity. Only for sources working very close to the ambient temperatures these problems can possibly be solved by the construction of extremely large cavity black-bodies [83]. However, the diameter of a high temperature standard is restricted to a few centimeters [65]–[75] by the requirement of uniform heating. As far as we know, no attempt has been made to verify Planck's radiation formula with the aid of optical cavity sources for wavelengths longer than the 52 μm considered by Rubens and coworkers [84], [85].

Diffraction losses in radiometry due to the finite radius R of circular apertures have been studied only recently by means of scalar diffraction theory valid for $\lambda \ll R$, i.e. for optical and near-infrared radiation [86]. For far-infrared and submillimeter radiation, the scalar plane wave theory [87] as well as the Kirchoff and 'improved' Kirchoff approximations are not sufficient [88]. The rigorous electromagnetic diffraction theory for finite apertures is very difficult. In the case of a circular aperture in a perfectly conducting screen, the exact transmission coefficient for plane waves at normal incidence is known for $2\pi R \leq 10\lambda$ [89], [90], i.e. for microwaves only. The only rigorous treatment of an extended light source known to the authors is the theory of the strip lamp of infinite length due to Facq [91]. The complete electromagnetic wave theory of a thermal cavity source typical for submillimeter waves with $d \approx 50\lambda$ is a hopeless task. For this reason, a *one-dimensional model* for the unclosed cavity source was developed [92], which displays all the typical features of a laboratory-size far-infrared black-body with a finite aperture. A detailed discussion is presented in a previous paper [93].

B. The mode density of the electromagnetic radiation

We now restrict our considerations to the case of the *closed* black-body cavity with *perfectly reflecting* walls. The asymptotic mode density $D_0(\nu)$ of the electromagnetic resonances in the lossless cavity (1.6) plays a dominant role in radiation physics:

(i) It is well known that $D_0(\nu)$ is a constituent of *Planck's radiation formula*. As a consequence, we find it involved in *Wien's displacement law*

$$\frac{h \nu_{max}}{k T} = 2.822, \quad (1.7)$$

where ν_{max} is defined by

$$\frac{d}{d\nu} \left(\frac{\nu D_0(\nu)}{\exp\left(\frac{h \nu}{k T}\right) - 1} \right) = 0, \quad (1.8)$$

as well as in the *Stefan-Boltzmann formula*

$$E_0(T, V) = \int_0^\infty \frac{h \nu D_0(\nu)}{e^{\hbar\nu/kT} - 1} d\nu = \frac{\pi^2 V(k T)^4}{15 (\hbar c)^2} \quad (1.9)$$

and in the thermodynamic properties of the photon gas [94]. The mode density appears in the *mean square fluctuation* of the radiation energy

$$\left(\frac{\Delta u}{u}\right)^2 = \frac{e^{\hbar\nu/kT}}{D_0(\nu) \Delta\nu} \quad (1.10)$$

[95]–[98]. Finally, we find $D_0(\nu)$ in the complex *coherence tensor* of the black radiation field [99]–[104],

$$\mathcal{E}_{ij}(\mathbf{r}, t) = 2 \int A(K) (K^2 \delta_{ij} - K_i K_j) e^{i(\mathbf{kr} - Kct)} d^3 \mathbf{K}, \quad (1.11)$$

where \mathbf{K} = wave vector, $K = 2\pi\nu/c$, and

$$A(K) = \frac{\hbar c}{V} \frac{D_0(K)}{2 K^3} \frac{1}{e^{\hbar c K/kT} - 1}. \quad (1.12)$$

The complex coherence tensor $\mathcal{E}_{ij}(\mathbf{r}, t)$ describes the correlations between the electric field vectors at the points \mathbf{r}_1 and $\mathbf{r}_2 = \mathbf{r}_1 + \mathbf{r}$ and times t_1 and $t_2 = t_1 + t$ in a cavity filled with black-body radiation. The coherence tensor \mathcal{H}_{ij} is defined in an analogous manner.

(ii) According to the principles of detailed balance, the radiation equilibrium between any pair of energy levels of a material system is maintained by means of a balance between the rates of spontaneous emissions and induced emission and induced absorption. At thermal equilibrium we have [105]

$$A = B h \nu D_0(\nu) V^{-1} \quad (1.13)$$

where A and B are the *Einstein coefficients of spontaneous and stimulated emission*, respectively. By virtue of (1.13), $D_0(\nu)$ influences the laser action as well as the fluorescence life-time.

(iii) In Welton's theory, the *Lamb-shift* [106] of the H-atom is represented by

$$\Delta E = \frac{Z^4}{3 \pi^2} \frac{R y \alpha^4 h c^4}{n^3} \int_{\nu_1}^{\nu_2} D_0(\nu) V^{-1} \nu^{-3} d\nu, \quad (1.14)$$

with

$$\nu_1 \approx \frac{Z^2 c^2}{h r_0^3 n^3}, \quad \nu_2 \approx \frac{m_0 c^2}{2 \pi h} \quad (1.15)$$

and thus depends on $D_0(\nu)$ as well.

Past [33], [107] and present [108] studies of the black-body radiation are based on the assumptions (1.4), which are equivalent to the requirement $V \rightarrow \infty$ or the *free-space limit*. For *finite* cavities, size and shape dependent modifications of the mode density $D_0(\nu)$ are required. In particular, the thermal radiation in a closed cavity of finite volume is not necessarily unpolarized, homogeneous, and isotropic. Larger deviations from the free-space limit may occur for narrow-band phenomena, i.e. the single mode laser. Corrections of the spontaneous emission rate have already been predicted for two simple non-free-space situations, viz. in the vicinity of a perfectly reflecting mirror and in a Fabry-Perot resonator [109]. Experimental evidence for boundary-wall effects has been found in the measurement of the fluorescence lifetime [110].

For these and other reasons the electromagnetic mode density in a finite lossless cavity seems worthwhile studying. In the following sections, the precise mathematical formulation of the problem as well as a survey of the state of the art are given. Surface-area dependent corrections are the subject of section 4, whereas second and higher order corrections are considered in the sections 5 to 8. The according refinements of the above formulae are studied in the sequel.

2. Electromagnetic Modes in an Ideal Cavity Resonator

A. The electromagnetic boundary value problem

An 'ideal' resonator is represented by an empty closed cavity with perfectly reflecting walls. The free electromagnetic oscillations \mathbf{E} , \mathbf{H} , obey the vector Helmholtz equation

$$(\nabla^2 + K^2) \begin{Bmatrix} \mathbf{E} \\ \mathbf{H} \end{Bmatrix} = \mathbf{0} \quad (2.1)$$

and the divergence conditions

$$\nabla \cdot \mathbf{E} = 0, \quad \nabla \cdot \mathbf{H} = 0 \quad (2.2)$$

throughout the interior region of the cavity, and the boundary conditions

$$\mathbf{n} \times \mathbf{E} = \mathbf{0}, \quad \mathbf{n} \cdot \mathbf{H} = 0 \quad (2.3)$$

on the enclosing walls [111]–[114]. Let the interior region G be a bounded, open, connected set with the boundary F in the Euclidean space R^3 with the volume V and the surface area S . Assuming the existence of a continuous third derivative on F , Müller and Niemeyer [115] have demonstrated 1961 that the above problem possesses an infinite number of eigenfrequencies $\nu_n = K_n c/2 \pi$. The ν_n are real, have no finite accumulation point, and show finite degeneracy. The case $\nu = 0$ is excluded, and we are entitled to write $0 < \nu_1 \leq \nu_2 \leq \nu_3 \leq \dots$. The corresponding eigenfunctions \mathbf{E}_n and \mathbf{H}_n form complete orthonormal sets. They are continuous in $G = G \cup F$ and have continuous derivatives in G . The rigorous Hilbert space operator theory of the problem is presented in Ref. [116]. The field vectors can be written in terms of two scalar potentials [117]–[119]. For simple cavity geometries with smooth or piecewise

smooth boundary surfaces the normal modes are known [113]–[115]. Examples are the parallelepiped, the circular cylinder, and the sphere. For complicated geometries, computational procedures exist at least for the numerical determination of the lowest modes [120], [121].

For our investigations of the surface terms in Section 4 we need the related *scalar* boundary value problems as well: The oscillations u obey the scalar wave equation in G ,

$$(\nabla^2 + K^2) u = 0 \quad (2.4)$$

and satisfy on F the *Dirichlet* condition

$$u = 0 \quad (2.5)$$

or the *Neumann* condition

$$\frac{\partial}{\partial n} u = 0, \quad (2.6)$$

with $G \subset R^n$, $n = 2$ or 3 . The rigorous proof of the existence of the complete system of eigenfunctions u_n with the corresponding eigenvalues K_n for this and similar ‘regular’ elliptic boundary value problems was given as late as 1953 by Gårding [122].

B. The degeneracy of the eigenvalues and the fluctuation of the mode density

We denote the number of modes with frequencies ν_n not exceeding ν by $N(\nu)$. Precisely,

$$N(\nu) = \sum_{\nu_n < \nu} G_n + \sum_{\nu_n = \nu} \frac{G_n}{2}, \quad (2.7)$$

where $G_n = G(\nu_n)$ is the finite weight or degeneracy of the resonance ν_n . Subsequently the eigenvalue density $D(\nu)$ may be defined by

$$D(\nu) = \frac{d}{d\nu} N(\nu). \quad (2.8)$$

Strictly speaking, $D(\nu)$ is not a smooth function, but a sum of distributions $\delta(\nu - \nu_n)$, and $N(\nu)$ is a step function, the spectrum being discrete. For three simple cavity shapes, a small portion of the weight distribution obtained by a computer programm is shown in Figure 1. The reduced frequency

$$\Omega = 2 V^{1/3} \frac{\nu}{c}, \quad (2.9)$$

is introduced in order to compare the different geometries, i. e. the sphere, the cube, and the circular cylinder with the diameter-to-length ratio $2 \pi^{-1/2}$. The weight is plotted as a function of Ω^2 near $\Omega = 100$ with the sampling intervall $\Delta(\Omega^2) = 1$. This is the natural eigenvalue distance of the cube (see Section 5).

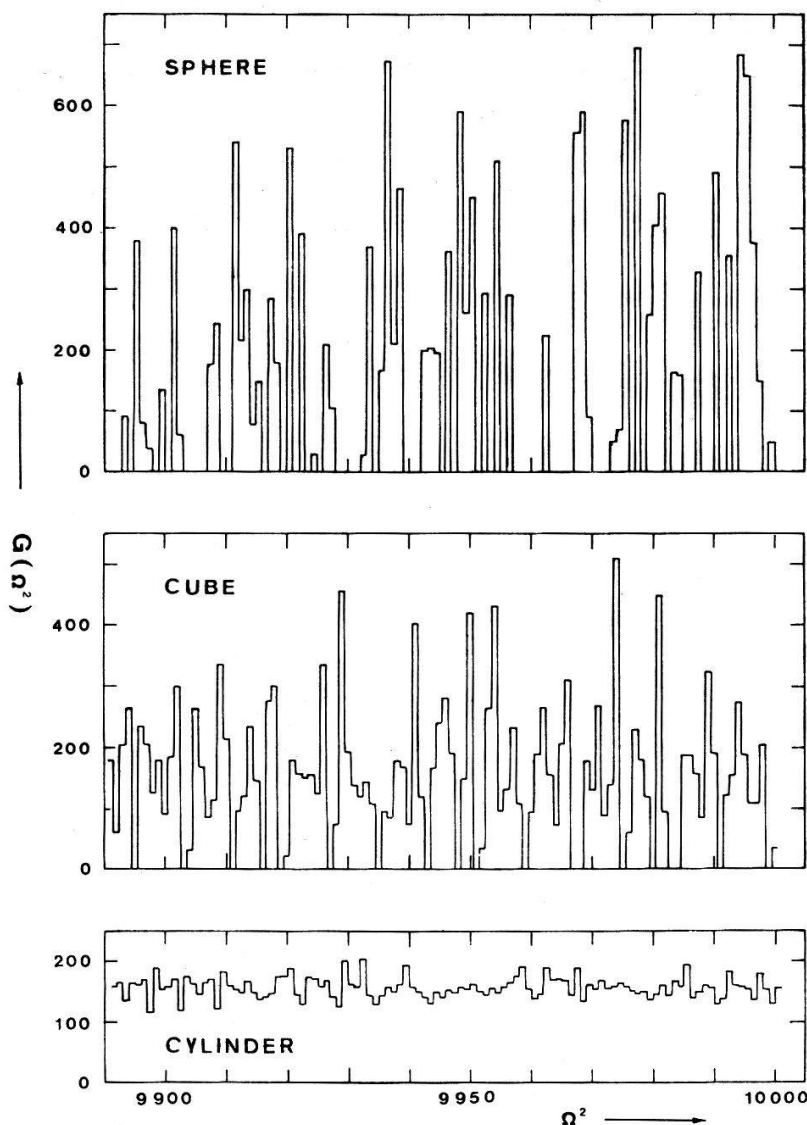


Figure 1

The weights of the cavity resonances are presented for the *sphere*, the *cube*, and the *cylinder* with radius/length $= \pi^{-1/2}$, near $\Omega^2 = 10^4$. $\Omega = 2 V^{1/3}/\lambda$ is the reduced wavenumber with V = volume of the resonator. For the cube, the squared reduced eigenvalues Ω_n^2 are integers, and the degeneracies $G = G_n$ are well defined. For the sphere and the cylinder, $G = G(\Omega^2 + 1/2)$ defined as the number of eigenvalues between Ω^2 and $\Omega^2 + 1$ is used.

Large fluctuations appear in the weight spectrum which evidently depend on the degeneracy of the eigenvalues due to the symmetry of the cavity. For the spherical cavity, each mode of 'angular quantum number' l gives rise to a $2(2l+1)$ -fold degeneracy. For the cube-shaped resonator, most modes have the weight 12 plus 'accidental' degeneracy (see 5, B. 2). The degeneracy is only 2 for most of the normal modes inside the circular cylinder. Our computations demonstrate that a fluctuating part of the density $D(\nu)$ with an amplitude proportional to ν survives even in the case of large frequencies (see 5 and 6).

C. Averaging procedures

In order to eliminate the fluctuations and to obtain a smooth density, the following procedures can be used:

(i) *Repeated integration* [123]. Instead of the $D(\nu)$, the $N(\nu)$ or even the integral over $N(\nu)$ are calculated. The smoothed density is recovered by differentiation. This method is used for the parallelepipeds (see Section 5 and Fig. 3 to 6).

(ii) *Square smoothing* [93]. $D(\nu)$ is replaced by

$$D(\nu; \Delta\nu) = \sum_n G_n f(\nu_n, \nu; \Delta\nu), \quad (2.10)$$

where

$$f(\nu_n, \nu; \Delta\nu) = \begin{cases} (\Delta\nu)^{-1} & \text{for } |\nu_n - \nu| < \frac{\Delta\nu}{2} \\ (2\Delta\nu)^{-1} & \text{for } |\nu_n - \nu| = \frac{\Delta\nu}{2} \\ 0 & \text{for } |\nu_n - \nu| > \frac{\Delta\nu}{2} \end{cases}. \quad (2.11)$$

Then the averaged density $\bar{D}(\nu)$ is recovered by the relation

$$D(\nu; \Delta\nu) = \int_{\nu - \Delta\nu/2}^{\nu + \Delta\nu/2} \bar{D}(\tilde{\nu}) d\tilde{\nu}. \quad (2.12)$$

Thus, $\bar{D}(\nu)$ is by definition the function giving the same smoothed density $D(\nu; \Delta\nu)$ as the distribution $D(\nu)$. The procedure is used for the cylindrical cavities in Section 6 (see Fig. 7 and 9).

(iii) *Lorentzian smoothing*. This method is similar to (ii), but f is replaced by the well-known Lorentz shape function with the width $\Delta\nu$, see Ref. [124], [125].

(iv) *Log Gaussian smoothing* is defined in appendix A II. See Ref. [126].

(v) *Integral transforms*. Parameter depending summations of the form

$$F(t) = \sum_n G_n f(\nu_n, t), \quad (2.13)$$

are carried through without reference to the density at all. Typically,

$$f(\nu_n, t) = e^{-(2\pi\nu_n/c)^2 t}, \quad (2.14)$$

used in appendix A.1, or

$$f(\nu_n, t) = \frac{\nu_n}{(e^{\nu_n/t} - 1)}, \quad (2.15)$$

applied in Ref. [127] are considered, which correspond to the Laplace- and Lambert-transforms respectively. (2.15) leads directly to the total radiation energy of the cavity discussed in Section 10.

The averaging procedures (i) and (ii) are most simple if the density is evaluated by computer counting of the eigenvalues. The appropriate averaging procedure, if any, depends on the physical problem to be solved. In the procedure (ii) and (iii), $\Delta\nu$ plays the role of the *bandwidth* or *spectral resolution*. For spectroscopic applications, the slit function of the monochromator combined with the oscillator mean energy

ought to be used. If narrow band phenomena are studied, the average density is more or less meaningless. The procedures (ii) and (iii) may be applied using relatively small $\Delta\nu$. The fluctuations can be described by the relative mean deviation [93],

$$\overline{\delta}(\nu; \Delta\nu) = \frac{\overline{|D(\nu; \Delta\nu) - \overline{D}(\nu)|}}{\overline{D}(\nu)}, \quad (2.16)$$

as a function of the spectral resolution $\Delta\nu$. The quantity (2.16) is calculated in Sections 5 and 6 in connection with the square smoothing.

3. Asymptotic Expansions of the Electromagnetic Mode Density - State of the Art

A. The Turn of the Century

The first counting of points in the \mathbf{K} -space seems to be due to Pockels [128] and dates back to 1891. About 1905, Jeans [129] and Rayleigh [130] introduced the concept of the mode density into the theory of black-body cavity radiation. For a parallelepiped cavity, Jeans obtained

$$N(\nu) \approx N_0(\nu) = \frac{8\pi}{3} V \left(\frac{\nu}{c} \right)^3, \quad (3.1)$$

valid for sufficiently large values of $V(\nu/c)^3$. This result was verified for other simple cavity geometries in a Leiden dissertation by Miss Reudler. About 1911 Weyl [131], [132] proved that (3.1) is asymptotically exact for $V(\nu/c)^3 \rightarrow \infty$ irrespective of the shape of the cavity. He applied the theory of integral equations Hilbert [133] had developed a few years before. A modern account of these methods is found in Ref. [134]. A few historic details can be read in Kac's lecture 'Can one hear the shape of a drum' [135]. For longer wavelengths and finite cavity volumes, (3.1) is only a crude approximation. Correction terms are required which may *depend on the shape* of the resonator. A priori, one may expect (3.1) to be the first term of an asymptotic expansion:

$$N(\nu) \sim N_0(\nu) + N_1(\nu) + N_2(\nu) + \dots \quad (3.2)$$

N_1 may be thought to be proportional to the surface area S and to the second power of the frequency, N_2 to a linear dimension and to the first power of the frequency. The first note on the related long-wave black-body problem is found in Planck's edition of Kirchoff's papers [136] which appeared in 1898¹⁾.

The first error estimate of (3.1) was presented 1913 in Weyl's third paper [137] on cavity radiation. It reads

$$-a \left(\frac{\log N}{N^{1/3}} \right)^{1/2} \leq \left(\frac{2\pi\nu_n}{c} \right)^2 - \left(\frac{3\pi^2 N}{V} \right)^{2/3} \leq a' \frac{\log N}{N^{1/3}}, \quad (3.3)$$

¹⁾ «Die Schwierigkeit liegt darin, dass im allgemeinen Falle die auf einen Körper auffallenden Wellen nicht unabhängig sind vom Körper selbst. Letzteres wird zwar gewöhnlich stillschweigend als zutreffend angenommen, es ist aber nur dann richtig, wenn die Wellenlängen verschwindend klein sind gegen die Krümmungsradien aller Körperoberflächen».

for the error of the N -th eigenvalue. Here, a and a' are positive constants. Actually, Weyl found a factor $2 \pi^2$ instead of $3 \pi^2$ in the asymptotic value of $(2 \pi \nu_N/c)^2$ because he considered the elastic oscillation problem. Therefore he was counting longitudinal modes as well. From (3.3) we easily conclude

$$N(\nu) - N_0(\nu) \sim \mathcal{O}((\nu^5 \log \nu)^{1/2}). \quad (3.4)$$

We shall see that this estimate is true, although Weyl's proof does not necessarily apply to the electromagnetic problem.

B. The Carleman methods

The methods of Weyl and Courant were not sufficiently powerful to give more information than found in (3.1) and (3.4). In 1934, Carleman [138], [139] introduced Tauberian procedures reminiscent of analytic number theory into the study of asymptotic distributions. The essential steps are:

- (i) A set $\{T_t\}$ of operators is studied instead of the differential operator T with $T u = K^2 u$.
- (ii) The Green kernels $f_t(\mathbf{x}, \mathbf{y})$ for $\{T_t\}$ are constructed.
- (iii) The dependence of $f_t(\mathbf{x}, \mathbf{y})$ upon t and particularly the asymptotic behaviour are investigated.
- (iv) An appropriate Tauberian theorem yields the asymptotic behaviour of the eigenfunctions and the eigenvalues.

For illustration, the indication of an elegant proof of Weyl's theorem (3.1) by a Carleman procedure based on the Tauberian theorem due to Hardy, Littlewood, and Karamata [140], is given in the appendix A.1.

About ten years ago, the Carleman methods were applied to the electromagnetic boundary value problem. Müller and Niemeyer [115] proved

$$N(\nu) - N_0(\nu) \sim o(\nu^3). \quad (3.5)$$

In a subsequent paper, Niemeyer [141] obtained the refined result

$$N(\nu) - N_0(\nu) \sim \mathcal{O}(\nu^2 \log \nu) \quad (3.6)$$

as well as some asymptotic relations for the electric field vector. Further refinements of the error estimate are obtained if the fluctuating part of the eigenvalue distribution is smoothed by one of the averaging procedures defined in 2.C.

C. Average error estimates

Using Lorentzian smoothing, Balian and Bloch [125] have shown recently that there is no first order average correction term proportional to the surface area S of the cavity:

$$N_1 = \text{const} \nu^2 S = 0. \quad (3.7)$$

This vanishing of the surface term is peculiar to the electromagnetic vector problem. In Section 4 we present a detailed study of the surface term, including a less general,

but constructive proof of (3.7). For resonators with *smooth* boundary surfaces, Balian and Bloch obtain the average result

$$N_2 = b \left(\frac{\nu}{c} \right), \quad (3.8)$$

in the limit of a narrow bandwidth, i.e. $(\Delta\nu/2)^2 \ll \nu^2$. The constant b is related to the main curvature radii R_1 and R_2 at each point of the boundary surface S by the formula

$$b = \frac{1}{3\pi} \int_S (R_1^{-1} + R_2^{-1}) dS. \quad (3.9)$$

The methods used by these authors fail for cavities with *sharp edges and corners*. In Sections 5 to 8 we study N_2 for a number of resonator geometries with non-smooth surfaces. Furthermore, we think that the sign as well as the modulus of the constant b determined by Balian and Bloch are incorrect. This is discussed in Section 7.

The only result actually available for a piecewise smooth cavity surface was derived recently by Case and Chiu [127]. The authors consider the *cube shaped resonator* with the edge length L and determine the total radiation energy by direct summation using the Poisson summation formula. The result is the expansion

$$\begin{aligned} E(T) &\sim E_0(T) + E_1(T) + E_2(T) + \dots \\ &= \frac{\pi^2}{15} \frac{(kT)^4}{(\hbar c)^3} L^3 - \frac{\pi}{4} \frac{(kT)^2}{\hbar c} L + \frac{1}{2} kT \\ &\quad - 0.097 \hbar c L^{-1} + \mathcal{O}(e^{-4\pi kTL/\hbar c}), \end{aligned} \quad (3.10)$$

valid for sufficiently large L/T . As expected, the infinite-space term E_0 corresponds to the Stefan-Boltzmann formula. The above result agrees with (3.7) in so far as the surface term $E_1 = \text{const} L^2 T^3$ vanishes. However, the first non-vanishing correction E_2 has the *opposite sign* of the term N_2 given in the relations (3.8) and (3.9).

D. The scalar problem

Here we should like to mention the much more advanced results of the scalar problems (2.4/5) and (2.4/6). As references, we suggest to the reader the review by Clark [142], the papers of Pleijel [143] and Brownell [126] as well as the most recent investigations by Balian and Bloch [124], Hilf [144], Stewartson and Waechter [145]. In physics, the scalar Dirichlet mode density is applied to the elastic vibrations of a membrane ('drum') and to the Fermi gas model of the nuclei [146], [147].

For one dimension, the relations $N_{\text{scalar}}^I(\nu) \sim \text{const} \nu$ and $N_{\text{elmag}}^I(\nu) = 0$ hold.

For two dimensions, Brownell [126] found

$$N_{\text{scalar}}^{II}(\nu) \sim \pi \sigma \left(\frac{\nu}{c} \right)^2 \mp \frac{1}{2} \gamma \left(\frac{\nu}{c} \right) + \frac{1}{6} + \tilde{\mathcal{O}}(\nu^{-\eta} \log \nu), \quad (3.11)$$

for a *smooth* boundary curve of length γ . The area of the two-dimensional domain is denoted by σ . η obeys $0 < \eta \leq 1$. The symbol $\tilde{\mathcal{O}}$ indicated that the expansion is valid

in the log Gaussian average (see Appendix 2.B). For a *square* shaped domain with the edge length L the expansion reads

$$N_{\text{scalar}}^{\text{square}}(\nu) \sim \pi L^2 \left(\frac{\nu}{c}\right)^2 \mp 2 L \left(\frac{\nu}{c}\right) + \frac{1}{4} + \tilde{\mathcal{O}}(\nu^{-r}), \quad (2.12)$$

where r is an arbitrary positive real number. In both expansions, the minus sign applies to the Dirichlet, the plus sign to the Neumann problem. The third term in the above formulae combines metric and topological features of the domain: Brownell determined 1/6 for a smooth boundary and proved that 1/48 must be added for each rectangular corner of the square. Thus $1/6 + 4/48 = 1/4$ is obtained. The most advanced results known so far were recently derived for the circle [145]. They include six terms of an expansion of the type (2.13/14).

For three dimensions, Brownell found

$$N_{\text{scalar}}^{\text{III}}(\nu) \sim \frac{4}{3} \pi V \left(\frac{\nu}{c}\right)^3 \mp \frac{1}{4} \pi S \left(\frac{\nu}{c}\right)^2 + \frac{1}{6 \pi} \int_S (R_1^{-1} + R_2^{-1}) dS \left(\frac{\nu}{c}\right) + \tilde{\mathcal{O}}(\nu^{1-\eta} \log \nu), \quad (3.13)$$

for a *smooth* boundary surface with the area S . For the cube shaped domain he obtained

$$N_{\text{scalar}}^{\text{cube}}(\nu) \sim \frac{4}{3} \pi L^3 \left(\frac{\nu}{c}\right)^3 \mp \frac{3}{2} \pi L^2 \left(\frac{\nu}{c}\right)^2 + \frac{3}{2} L \left(\frac{\nu}{c}\right) \mp \frac{1}{8} + \tilde{\mathcal{O}}(\nu^{-r}). \quad (3.14)$$

We observe that *surface terms* appear in the above expansions. They are absent in the corresponding relation for the electromagnetic vector problem. This illustrates that the electromagnetic problem cannot be reduced to the scalar problems by a naive procedure. This connection is investigated in Sections 4 and 5. The term (3/2) $L(\nu/c)$ in (3.14) cannot be derived from the curvature term in (3.13) by approaching infinitesimal radii of curvature: An erroneous coefficient 1 is obtained instead of 3/2. According to Balian and Bloch [124] the existence of sharp edges is ‘pathological’.

4. The Surface Area Dependent Terms of Partial Mode Densities

A. *E*- and *H*-type mode densities

According to (3.7) and 3.10) the surface term of the averaged *total* mode density $D(\nu)$ vanishes. However, surface terms are obtained if *E*- and *H*-type modes (TM and TE resonances) are counted separately, i.e. if the *partial* densities $D_E(\nu)$ and $D_H(\nu)$ are studied. Physical consequences are (i) a first order anisotropy correction of the radiation field, and (ii) the surface terms of the temporal autocorrelation functions of the field components studied in Section 11.

The separation into *E*- and *H*-type modes stems from the fact that the solutions of the electromagnetic wave equation (2.1) can be represented in terms of two scalar

wave potentials in a region that is homogeneous, isotropic, and free from electric and magnetic polarizations. The z -components of the Hertzian vector,

$$u_E = \prod_{E,z}, \quad u_H = \prod_{H,z}, \quad (4.1)$$

show this property [117]–[119]. Let us assume a boundary geometry that allows a separation of the wave equation in terms of orthogonal curvilinear coordinates (x_1, x_2, x_3) with $h_3 = 1$ and h_1/h_2 independent of x_3 in the usual notation (see e.g. Ref. [113], p. 7). Consequently, two independent sets of solutions are obtained as follows:

$$\left. \begin{aligned} \mathbf{E}_E &= (h_1 \partial_3 \partial_1, h_2 \partial_3 \partial_2, \partial_3^2 + K^2) u_E, \\ \mathbf{H}_E &= i \omega \epsilon (h_2 \partial_2, -h_1 \partial_1, 0) u_E, \end{aligned} \right\} \quad (4.2)$$

$$\left. \begin{aligned} \mathbf{E}_H &= i \omega \mu (-h_2 \partial_2, h_1 \partial_1, 0) u_H, \\ \mathbf{H}_H &= (h_1 \partial_3 \partial_1, h_2 \partial_3 \partial_2, \partial_3^2 + K^2) u_H, \end{aligned} \right\} \quad (4.3)$$

where $\partial_n = \partial/\partial x_n$, $i^2 = -1$, $\epsilon u = c^{-2}$, and where $\omega = 2\pi\nu$ is the eigenfrequency of the mode with $\nu = \nu_E$ or $\nu = \nu_H$ respectively. The E -type density is defined as

$$D_E(\nu) = \frac{d}{d\nu} N_E(\nu), \quad (4.4)$$

with

$$N_E(\nu) = \sum_{\nu_{E,n} < \nu} G(\nu_{E,n}) + \frac{1}{2} \sum_{\nu_{E,n} = \nu} G(\nu_{E,n}). \quad (4.5)$$

The definition of $D_H(\nu)$ is analogous. The total density is

$$D(\nu) = D_E(\nu) + D_H(\nu). \quad (4.6)$$

To our knowledge, the E - and H -type mode densities were never studied separately.

B. Asymptotic surface terms

Examples of geometries leading to (4.2/3) are the cylinder with $E_3 = E_z$ and the sphere with $E_3 = E_r$. Let us denote by S_{\perp} the total area of those parts of the boundary surface which are orthogonal to the field components E_3 and H_3 , and by $S_{\parallel} = S - S_{\perp}$ the remaining surface area. For cylinders, S_{\perp} includes the 'shorting plates'. Hence we find $S_{\perp} = 2\pi R^2$ and $S_{\parallel} = 2\pi R L$ for circular cylinders with radius R and length L . For a sphere, $S_{\perp} = 4\pi R^2$ is the whole surface area, whereas $S_{\parallel} = 0$. After some calculation, we find from the field equations (4.2/3) that the boundary conditions (2.3) are satisfied if

$$u_E = 0 \quad \text{on} \quad S_{\parallel}, \quad \frac{\partial}{\partial n} u_E = 0 \quad \text{on} \quad S_{\perp}, \quad (4.7)$$

$$u_H = 0 \quad \text{on} \quad S_{\perp}, \quad \frac{\partial}{\partial n} u_H = 0 \quad \text{on} \quad S_{\parallel}. \quad (4.8)$$

We have thus decomposed the vector wave problem (2.1–3) into the two scalar problems (2.4/4.7) and (2.4/4.8) with mixed boundary conditions. These two problems are *complementary*: u_E has to fulfil the *Dirichlet* condition on those smooth pieces of the surface where u_H obeys the *Neumann* condition, and vice versa. In order to obtain the asymptotic expansions including the surface terms, we construct the image-type Green functions

$$f_{t,E}(\mathbf{x}, \mathbf{y}) = f_{t,0}(\mathbf{x}, \mathbf{y}) - f_{t,0}(\mathbf{x}, \mathbf{y}_{\parallel}) + f_{t,0}(\mathbf{x}, \mathbf{y}_{\perp}), \quad (4.9)$$

$$f_{t,H}(\mathbf{x}, \mathbf{y}) = f_{t,0}(\mathbf{x}, \mathbf{y}) + f_{t,0}(\mathbf{x}, \mathbf{y}_{\parallel}) - f_{t,0}(\mathbf{x}, \mathbf{y}_{\perp}). \quad (4.10)$$

Here, \mathbf{y}_{\parallel} and \mathbf{y}_{\perp} are image points outside S_{\parallel} and S_{\perp} , respectively. $f_{t,0}(\mathbf{x}, \mathbf{y})$ is defined in (A.4), Appendix A 1. Evidently, $f_{t,E}$ and $f_{t,H}$ fulfill the boundary conditions (4.7) and (4.8), respectively. With the aid of these functions we find that each smooth piece S' of the surface contributes to the surface terms of the mode densities D_E and D_H according to the expansion (3.13), i. e. $\mp (\pi/2) S' \nu/c^2$. Thus we obtain

$$D_E(\nu) \sim \frac{1}{2} D_0(\nu) + \frac{\pi}{2} (S_{\perp} - S_{\parallel}) \frac{\nu}{c^2} + \overline{\mathcal{O}}(1), \quad (4.11)$$

$$D_H(\nu) \sim \frac{1}{2} D_0(\nu) - \frac{\pi}{2} (S_{\perp} - S_{\parallel}) \frac{\nu}{c^2} + \overline{\mathcal{O}}(1). \quad (4.12)$$

Because these results are valid only in the average, the notation $\overline{\mathcal{O}}$ is introduced. The contribution of any *edges* of the boundary surface would be of second order and can be disregarded.

From (4.11) and (4.12) we conclude

$$D_E(\nu) - D_H(\nu) \sim \pi (S_{\perp} - S_{\parallel}) \frac{\nu}{c^2}, \quad (4.13)$$

as well as

$$D(\nu) = D_E(\nu) + D_H(\nu) \sim D_0(\nu) + \overline{\mathcal{O}}(1). \quad (4.14)$$

Thus the surface area dependent term in the asymptotic expansion of the complete mode density $D(\nu)$ vanishes as a consequence of the ‘duality’ (4.7/8) found in the two basic scalar problems. We should point out that our proof is valid for all the boundary geometries allowing the separation discussed in 4.A. The expansion (4.14) is consistent with the result (3.7) proved by Balian and Bloch [125] as well with a conjecture due to Case and Chiu [127]. Furthermore, we shall find below (sections 5–8) that (4.14) agrees with all our computer results on finite frequency ranges. We observe that an *erroneous surface term* appears in $D(\nu)$ if the expansion (3.13) valid for the *scalar* problem is used for the *electromagnetic vector* problem in a naive manner. Therefore it is unlikely that the theory of perfect quantum gases of particles with non-zero mass in a finite volume developed by Hilf [144] does not apply to the radiation field in small cavities at low temperatures.

We emphasize that the theorems (4.13) and (4.14) hold for cone shaped cavities as well, because the single *L*-type solution [113] due to the sharp point of the cone contributes less than $\overline{\mathcal{O}}(1)$. From the theorem (4.13) we learn that special cavity shapes

exist where even $D_E(\nu)$ and $D_H(\nu)$ have vanishing surface terms, i.e. $D_E(\nu) - D_H(\nu) \sim \mathcal{O}(1)$. As examples we mention the circular cylinder with $R = L$, the square prism with $L = 2L_3$, and the spherical sector showing a half-angle near (not exactly) $\pi/4$. The notation is explained in Figure 2.

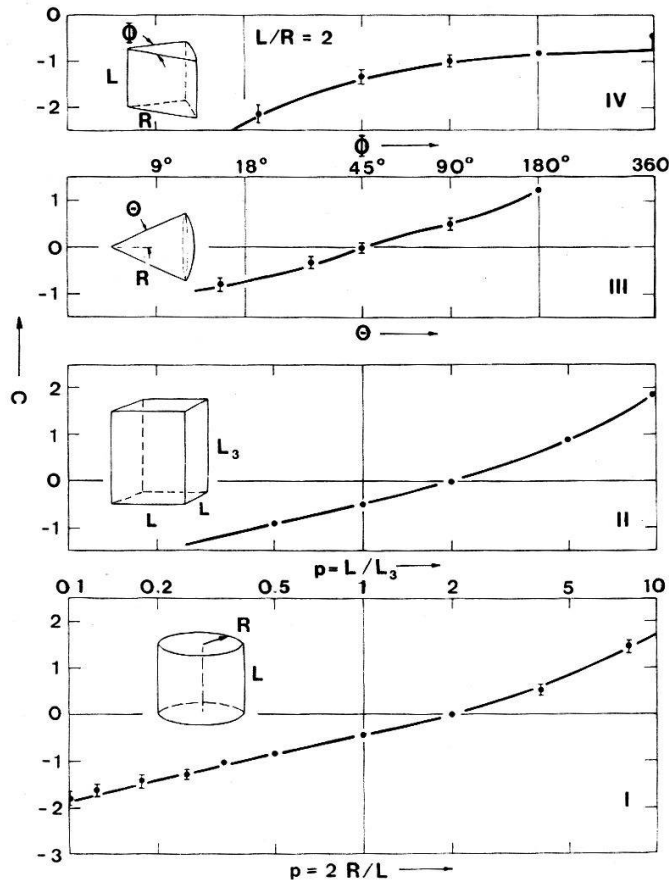


Figure 2

The coefficient C of the *first order relative mode density difference* $[D_E(\Omega) - D_H(\Omega)]/D(\Omega) = C/\Omega$ with $\Omega = 2V^{1/3}/\lambda$ is plotted as a function of the appropriate geometric parameter of the cavity for (I) *circular cylinders*, (II) *square prisms*, (III) *spherical sectors (cones)*, (IV) *sectors of cylinders (wedges)* with $2R = L$. The sphere and the hemisphere appear in (III) for $\theta = 180^\circ$ and 90° , respectively. The full circular cylinder does not appear as a special case of (IV) for $\Phi \rightarrow 360^\circ$ because of the discontinuity of the problem. The full curves represent C as result of the asymptotic expansion (IV.15) with (IV.16-20). The black circles represent C as obtained from the computation of the first 10^6 eigenvalues.

We observe that the image-type Green function technique (4.9/10) is restricted to the surface term problem. It fails for the second order correction if the boundary surface has sharp edges or corners. Its further application to smooth boundary surfaces, e.g. the sphere, is discussed in Section 7.

C. Computer results for finite frequencies

In order to compare formula (4.13) with our computer results, we write in it terms of $\Omega = 2V^{1/3}\nu/c$, and we obtain

$$\frac{(D_E(\Omega) - D_H(\Omega))}{D(\Omega)} \sim C \Omega^{-1}, \quad (4.15)$$

with

$$C = \frac{(S_{\perp} - S_{||})}{4V^{2/3}}. \quad (4.16)$$

For the above mentioned geometries, the first-order coefficient C reads for the *square prism with $p = L/L_3$*

$$C = \left(\frac{1}{2}\right) (p^{2/3} - 2 p^{-1/3}), \quad (4.17)$$

circular cylinder with $p = 2 R/L$

$$C = \frac{1}{2} \pi^{1/3} \left(\left(\frac{p}{2}\right)^{2/3} - \left(\frac{p}{2}\right)^{-1/3} \right), \quad (4.18)$$

sectors of circular cylinders with $\Phi < 2\pi$

$$C = \frac{1}{4} \left(\frac{2}{\Phi}\right)^{2/3} \left[\left(\frac{p}{2}\right)^{2/3} \Phi - \left(\frac{p}{2}\right)^{-1/3} (2 + \Phi) \right], \quad (4.19)$$

spherical sectors (cones) $\theta \leq \pi/2$

$$C = \frac{\pi}{4} \frac{2(1 - \cos\theta) - \sin\theta}{\left[\frac{2\pi}{3} (1 - \cos\theta)\right]^{2/3}}. \quad (4.20)$$

sphere

$$C = \left(\frac{9\pi}{16}\right)^{1/3} = 1.2088 \dots \quad (4.21)$$

The above asymptotic values for C are compared with the corresponding computer results in Figure 2.

D. Conclusion

Strictly speaking, we are not entitled to read the expansion (4.15) as an equation for finite Ω . However, the comparison with our computer results for the above geometries shows that this expansion is already a good approximation of the averaged $D_E - D_H$ for $\Omega \gtrsim 5$. E.g. in the case of the *sphere* we find

$$C_{\text{computer}} = 1.20 \pm 0.02, \quad (4.22)$$

for $5 \lesssim \Omega \lesssim 250$ in excellent agreement with the asymptotic value (4.21). The details of the computation procedure are presented in the next sections.

5. Second and Higher Order Corrections for Parallelepiped Cavities

A. The degeneracy of the eigenvalues of the cube

The computation of the mode density is most easily done in the case of a cube shaped resonator. Let L denote the edge length of the cube. In terms of the parameter

$$W = \frac{2L}{\lambda} = \frac{2L\nu}{c}, \quad (5.1)$$

the resonances are given by

$$Q = W^2 = n_1^2 + n_2^2 + n_3^2, \quad (5.2)$$

where the n_i are integer numbers. It is sufficient to consider $n_i \geq 0$, because the negative integers produce no further linear independent solutions. According to Ref. [113], p. 133, we obtain non-vanishing E - and H -type modes for any set $(n_i, n_i > 0 \text{ for } i = 1, 2, 3)$. If, however, n_1 or n_2 is zero, then the E -type solution vanishes. If, on the other hand, $n_3 = 0$, then the H -type field is zero. If more than one of the n_i is zero, then both solutions vanish. Consequently, the multiplicities $G = G_E + G_H$ read as follows:

$$\left. \begin{aligned} G &= 2 & \text{if no } n_i \text{ is zero} \\ G &= 1 & \text{if one } n_i \text{ is zero} \\ G &= 0 & \text{if two or all of the } n_i \text{ are zero.} \end{aligned} \right\} \quad (5.3)$$

These are the degeneracies used by Case and Chiu [127]. For the computer calculations we can save time by the consideration of ordered sets $(n_i, 0 \leq n_1 \leq n_2 \leq n_3)$. The following table for ' $G_E + G_H = G$ ' is readily established:

	$n_1 < n_2 < n_3$	$n_1 < n_2 = n_3$	$n_1 = n_2 < n_3$	$n_1 = n_2 = n_3$	
$n_1 = 0$	$2 + 4 = 6$	$1 + 2 = 3$	0	0	(5.4)
$n_1 > 0$	$6 + 6 = 12$	$3 + 3 = 6$	$3 + 3 = 6$	$1 + 1 = 2$	

In the case of the scalar *Dirichlet* problem (2.4/5) studied by Hilf [148], [149] the degeneracies are

$$\begin{aligned} g &= 1 & \text{if } n_1 \cdot n_2 \cdot n_3 \neq 0, \\ g &= 0 & \text{if } n_1 \cdot n_2 \cdot n_3 = 0. \end{aligned} \quad (5.5)$$

Comparing (5.3) with (5.5), one can easily see that

$$N(W) = N_{elmag} = \sum_{n_1^2 + n_2^2 + n_3^2 < W^2} G(n_1, n_2, n_3) + \frac{1}{2} \sum_{n_1^2 + n_2^2 + n_3^2 = W^2} G(n_1, n_2, n_3) \quad (5.6)$$

and

$$2 N^{III}(W) = 2 N_{scalar}^{Dirichlet} = 2 \sum_{n_1^2 + n_2^2 + n_3^2 < W^2} g(n_1, n_2, n_3) + \sum_{n_1^2 + n_2^2 + n_3^2 = W^2} g(n_1, n_2, n_3), \quad (5.7)$$

differ by a first order (surface) term. (The factor 2 is due to the two branches of the solutions of the electromagnetic problem.) Therefore, Hilf's surface corrections found with (5.5) and (5.7) do not apply to the radiation problem.

Similarly, the well-known connection with the number of lattice points inside a μ -dimensional sphere of radius W ,

$$F_\mu(W) = \sum_{n_1^2 + \dots + n_\mu^2 < W^2} \frac{1}{2} + \sum_{n_1^2 + \dots + n_\mu^2 = W^2} \frac{1}{2}, \quad (5.8)$$

has to be re-examined. One finds

$$2 N^{III}(W) = \left(\frac{1}{4} \right) (F_3(W) - 3 F_2(W) + 3 F_1(W) - 1), \quad (5.9)$$

whereas

$$N(W) = \left(\frac{1}{4} \right) (F_3(W) - 3 F_1(W) + 2). \quad (5.10)$$

Because of $F_1(W) = 2 W$ we obtain the simple relation

$$N(W) = \left(\frac{1}{4} \right) F_3(W) - \left(\frac{3}{2} \right) W + \frac{1}{2}, \quad (5.11)$$

for the electromagnetic problem. The connection with F_μ and with the results of elementary number theory is studied in the appendix A 2.

B. Results for the cube

1. *Average correction terms.* With the help of the weight table (4.4) we computed the eigenvalue density of the cube. Because of the large fluctuations (see Fig. 1) we applied a repeated-integration smoothing procedure. For $Q = W^2 = 0, 1, 2, \dots, 10000$ we calculated

$$M(W^2) = M_0(W^2) + M_1(W^2) + M_2(W^2) + \dots = \sum_{\tilde{W}^2=0}^{W^2-1} N(\tilde{W}) + \frac{N(W)}{2}, \quad (5.12)$$

with N defined by (5.6), and similarly $\tilde{M} = M_E - M_H$. N and \tilde{N} are reconstructed by differentiation, $N = (d/dW^2) M(W^2)$. The result is

$$N(W) = \left(\frac{1}{4} \right) \left(\frac{4\pi}{3} \right) W^3 - \left(\frac{3}{2} \right) W + \frac{1}{2} + \text{osc.} \quad (5.13)$$

and

$$\tilde{N}(W) = - \left(\frac{\pi}{4} \right) W^2 + W - \frac{1}{4} + \text{osc.}, \quad (5.14)$$

where ‘osc.’ denotes an oscillatory term which yields in the average a contribution decreasing faster than some negative power of W . In terms of $M(W^2)$ and $\tilde{M}(W^2)$, the relative third order error estimates obtained by the computation are displayed in Fig. 3.

From (5.11) and (5.13) it is easily conjectured that

$$F_3(W) = \left(\frac{4\pi}{3} \right) W^3 + \text{osc.}, \quad (5.15)$$

i.e. the *first*, the *second*, and the *third* order term in the expansion of the arithmetical function F_3 *vanish* in the average. This represents a well-known result proved by Brownell [126] for the log Gaussian average in the asymptotic limit $W \rightarrow \infty$ (see A 2.C). Thus, our result (5.13) verifies for the finite domain $W \leq 100$ an asymptotic estimate known in principle. The precise numerical value $N_3 = 1/2$ has been ‘assigned’

with the help of (5.11/15), whereas $N_3 = -1/4$ is checked by taking the limit of the two-dimensional resonator (see 5.D).

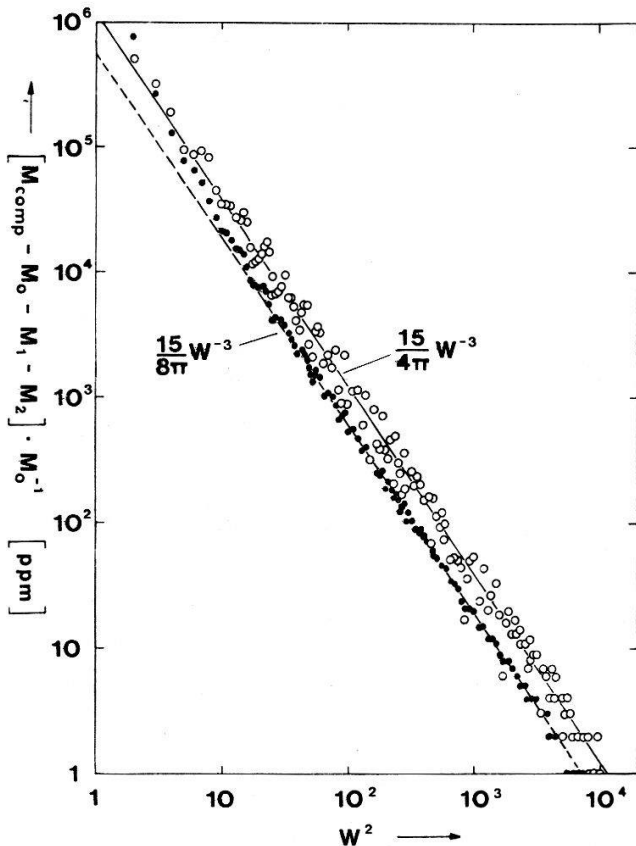


Figure 3
The cube shaped cavity with edge length L . The open and full circles represent the computer results for the third order corrections N_3 and \tilde{N}_3 , respectively, in terms of $M(W^2) = \int_0^{W^2} N(W^2) d(W^2)$ with $W = 2 L/\lambda$. The straight lines represent the asymptotic third order terms corresponding to $N_3 = 1/2$ and $\tilde{N}_3 = -1/4$.

2. *Fluctuating parts.* The remainder in the expansions (5.13/14) denoted by osc. allows for the large fluctuations of the eigenvalue density. These fluctuations can still be noticed in Figure 3, although the density is integrated twice. Actually, the degeneracy of most of the eigenvalues is higher than what might be expected from the table (5.4). In the Appendix A 2.C we show that the mean degeneracy is approximately $(3\pi/5)W$. From the computer results we learn that the fluctuating part of the mode density has a first-order 'amplitude'. It dominates the average second order correction unless a smoothing procedure is introduced. For bandwidth $c/L \leq \Delta\nu \leq 50 c/L$ we computed the relative mean deviation (2.16) using the square-smoothing method (2.10–12). We obtained

$$\overline{\delta}(\nu, \Delta\nu) \approx 0.1 c^2 L^{-2} \nu^{-1} (\Delta\nu)^{-1}. \quad (5.16)$$

C. Results for the square prism and the rectangular parallelepiped

1. *Averages.* We extended our computation to the *square prism* with the volume $L^2 \cdot L_3$ for values of the parameter $\dot{p} = L/L_3$ between 0.1 and 100. The following average expansions are found:

$$N(\nu) = N_0(\nu) - (2L + L_3) \left(\frac{\nu}{c} \right) + \frac{1}{2} + \text{osc.}, \quad (5.17)$$

$$\tilde{N}(\nu) = \tilde{N}_1(\nu) + 2L_3 \left(\frac{\nu}{c} \right) - \frac{1}{4} + \text{osc.}, \quad (5.18)$$

with \tilde{N}_1 as determined in Section 4. We point out that the constant terms $1/2$ and $-1/4$ do not depend on ρ . This is expected from the corresponding lattice-point considerations as well.

From (5.17/18) the expansion valid for the rectangular *parallelepiped* with edge lengths L_1, L_2, L_3 is easily conjectured:

$$N(\nu) = \frac{8\pi}{3} L_1 L_2 L_3 \left(\frac{\nu}{c}\right)^3 - (L_1 + L_2 + L_3) \left(\frac{\nu}{c}\right) + \frac{1}{2} + \text{osc.}, \quad (5.19)$$

$$\tilde{N}(\nu) = \pi(L_1 L_2 - L_2 L_3 - L_3 L_1) \left(\frac{\nu}{c}\right)^2 + 2 L_3 \left(\frac{\nu}{c}\right) - \frac{1}{4} + \text{osc.}, \quad (5.20)$$

2. *The oscillatory term for the flat square prism.* For flat square prisms ($\rho > 1$), the amplitude of the oscillatory term strongly increases with ρ , and the term is periodic in $W = 2L/\lambda$ with the period ρ . This is shown in Figure 4. Such a behaviour is understood qualitatively: Because of $W^2 = n_1^2 + n_2^2 + \rho_1^2 n_3^2$, flat cavities imply point lattices in the \mathbf{K} -space consisting of dense plane lattices which are well separated. The analysis of the computer results displayed in Figure 4 provides a simple formula describing the oscillatory term $M_4(W^2)$ for sufficiently large ρ and $W \gtrsim \rho$:

$$\frac{M_4(W^2)}{M_0(W^2)} \approx \left(\frac{\rho}{2}\right)^3 (W^2)^{-3/2} \cos \left[\frac{2\pi(W^2)^{1/2}}{\rho} + \frac{\pi}{2} \right]. \quad (5.21)$$

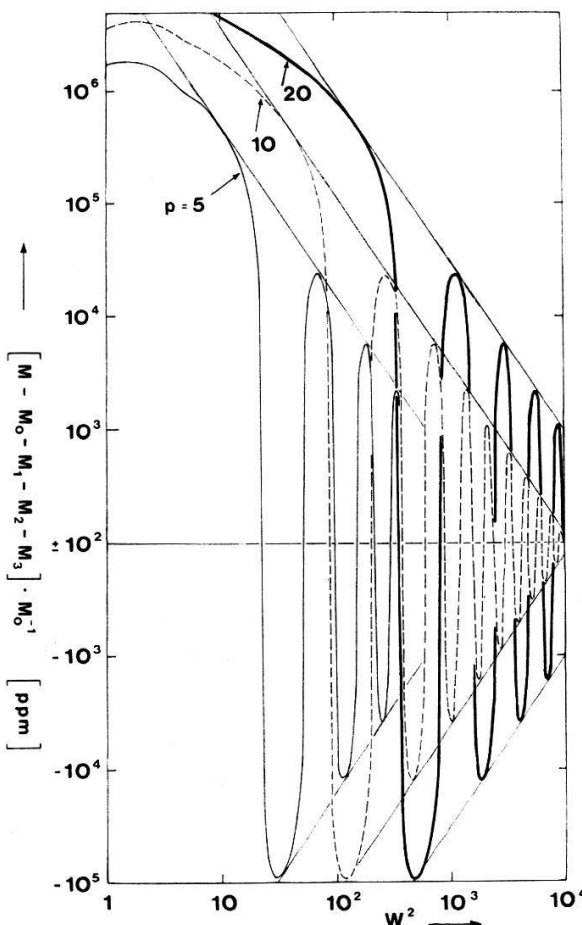


Figure 4

The *flat square prism* with edge lengths $L_1 = L_2 = L > L_3$. Computer results for the fluctuating part N_4 of the expansion obtained in terms of $M(W^2) = \int_0^{W^2} N(W^2) d(W^2)$, $W = 2L/\lambda$, are shown for various ratios $\rho = L/L_3$.

For $\rho = 5$ and $500 \leq W^2 \leq 1000$, the relation (5.21) and the computer results are compared in Figure 5. If we consider only the leading term, the differentiation yields the following fluctuating part of the mode density:

$$D_4(\nu) d\nu \approx 4 \frac{L^3}{L_3} \left(\frac{\nu}{c} \right) \sin \left[4 \pi L_3 \frac{\nu}{c} \right] \frac{d\nu}{c}. \quad (5.22)$$

This is valid for $L \gg L_3$ and $L_3 \gg \lambda/2$.

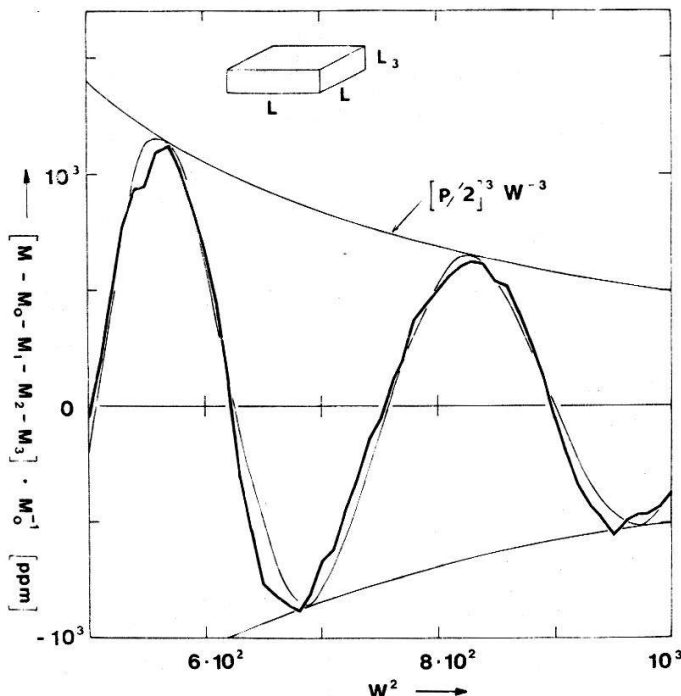


Figure 5

The flat square prism with edge lengths $L_1 = L_2 = L > L_3$. Computer results for the fluctuating term (heavy lines) are compared with the adapted function (5.21) (thin line), for the case $\rho = L/L_3 = 5$. The agreement increases with increasing ρ and $W = 2L/\lambda$. For the definition of M , consult caption of Figure 4.

D. The one- and two-dimensional limits

For very flat square prisms ($\rho \gg 1$) and for $W \lesssim \rho$, only the sets ($n_i, n_1 > 0, n_2 > 0, n_3 = 0$) produce eigenvalues. Accordingly, only the two-parameter set of E -type resonances with $G_E = 1$ survives. In the limit $L_3 \rightarrow 0$, the electromagnetic mode density becomes identical with the *two-dimensional scalar Dirichlet* mode density. Hence, we expect the expansion (3.12) to be valid for $L \gg L_3 \lesssim \lambda/2$.

This connection between the cavity radiation problem and the 'drum' problem is useful, because the eigenvalue distribution of the latter problem is known in detail [126], [135], [142], [145]:

(i) The accuracy of the computer program is easily checked by applying it to large values of the parameter ρ . Actually, our computation yields the Dirichlet version of the expansion (3.12) in the limit $W < \rho$. The relative error results leading to $N_2^{II}(\nu) = 1/4$ are given in Figure 6 in terms of $M(W^2)$.

(ii) The constants in the expansions of $N(\nu)$ and $\tilde{N}(\nu)$ obtained by numerical calculation can be interpreted and assigned a precise value by comparison with the two-dimensional limit. As a consequence of $N_H \rightarrow 0$ and $N_0 \rightarrow 0$, the formal relation

$$\lim_{L_3 \rightarrow 0} (N(\nu) + \tilde{N}(\nu)) = \lim_{L_3 \rightarrow 0} (2 N_E(\nu)) = N^{II}(\nu), \quad (5.23)$$

must hold. The factor 2 is due to the fact that lattice points on the $k_x - k_y$ -plane are counted with the weight 1/2 when considered as elements of an octant in three dimensions, but are counted with the full weight 1 when considered as elements of a quadrant in two dimensions. For the individual terms of the expansion, (5.23) implies the following requirements:

$$\left. \begin{aligned} N_1 + \tilde{N}_1 &\rightarrow \pi L^2 \left(\frac{\nu}{c} \right)^2, \\ N_2 + \tilde{N}_2 &\rightarrow -2 L \frac{\nu}{c}, \\ N_3 + \tilde{N}_3 &\rightarrow \frac{1}{4}. \end{aligned} \right\} \quad (5.24)$$

On the basis of these relations, the precise value $N_3 = -1/4$ can be assigned.

We observe that in the *one-dimensional limit* $L_3 \gg L \lesssim \lambda/2$ no eigenvalue W with $W < \rho$ exists. Hence $N(\nu) = 0$.

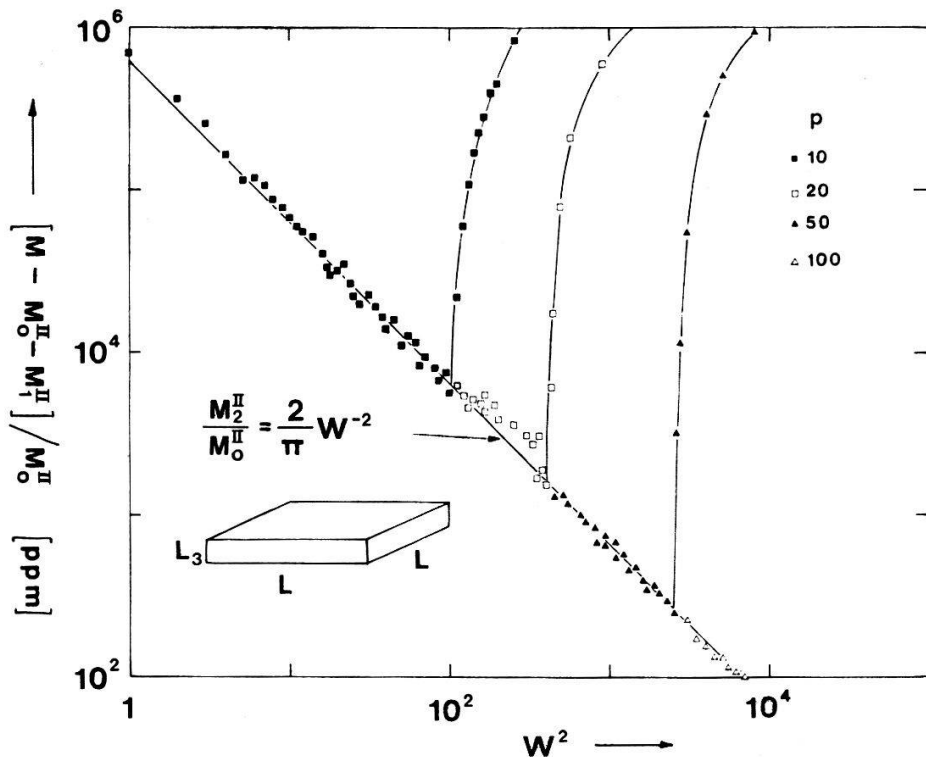


Figure 6

The *flat square prism* with edge lengths $L_1 = L_2 = L \gg L_3$ in the *two-dimensional limit*. Computer results (squares and triangles) are compared with the *asymptotic second order term* N_2^{II} in the expansion $N^{II} = N_0^{II} + N_1^{II} + N_2^{II} + \dots = (\pi/4) W^2 - W + 1/4 + \dots$, $W = 2 L/\lambda$, for the two-dimensional 'cavity', for the cases $p = L/L_3 = 10, 20, 50$, and 100 . We learn that N^{II} is valid for $L_3 \lesssim \lambda/2$. M as in Figure 4.

6. The Second Order Correction for Circular Cylinders and Their Sectors

A. The eigenvalue spectrum

The E - and H -type frequencies of the pill-box cavity are

$$\left(\frac{\nu}{c}\right)_{m,l,n}^E = \frac{1}{2\pi R} \left(j_{m,l}^2 + \left(\pi \frac{R}{L} n\right)^2\right)^{1/2}, \quad (6.1)$$

$$\left(\frac{\nu}{c}\right)_{m,l,n}^H = \frac{1}{2\pi R} \left(j_{m,l}'^2 + \left(\pi \frac{R}{L} n\right)^2\right)^{1/2}, \quad (6.2)$$

$j_{m,l}$ and $j_{m,l}'$ denote the 1th zero of the Bessel function J_m and its derivative J_m' , respectively, L the length, R the radius of the cylinder, $m, n = 0, 1, 2, \dots$, and $l = 1, 2, \dots$. The degeneracies $G_{E,H}(m, l, n)$ are discussed in the Appendix A 3. They can be summarized as follows:

m	n	G_E	G_H
0	0	1	0
0	> 0	1	0 if $l = 1$ 1 if $l > 1$
> 0	0	2	0
> 0	> 0	2	2

B. The computation of the mode density

1. *The eigenvalues.* We used two independent computer programmes based on the parameters $X = 2\pi R/\lambda$ and $W = 2L/\lambda$ respectively. Hence we computed the reduced squared frequencies

$$X_E^2(m, l, n) = j_{m,l}^2 + \left(\frac{\pi}{2} \rho n\right)^2 \quad (6.4)$$

and

$$W_E^2(m, l, n) = \left(\frac{\rho}{2\pi} j_{m,l}\right)^2 + n^2, \quad (6.5)$$

and the analogous reduced H -type resonances. By $\rho = 2R/L$ we denote the diameter-to-length ratio of the pill-box. We used the X - procedure for $\rho \geq 1/8$ and the W -procedure for $\rho \leq 2$. All the reduced eigenvalues with $W^2, X^2 \leq 10000$ were computed. This involves approximately 10^6 eigenvalues and 10^4 Bessel zeros. A few details of the calculations of the $j_{m,l}$ and $j_{m,l}'$ are presented in the Appendix A 4.

2. *The averaging.* Because of the low degeneracy, the fluctuations of the spectrum are weak, as is shown in Figure 1. Therefore, the square smoothing procedure (2.10-12) is sufficient. We varied the bandwidth $\Delta W, \Delta X$ between 2 and 100. For cavities of

usual laboratory size, this corresponds to spectral resolutions $\Delta(1/\lambda)$ between 0.1 and 10 cm^{-1} . The computer results are obtained in terms of

$$F_{comp}(W, \Delta W) = \frac{(D(W, \Delta W) - D_0)}{D_0}, \quad (6.6)$$

for $W = 0, 1, 2, \dots, 100 - \Delta W/2$. The constant C of the average relative second order correction is defined by

$$\frac{D - D_0}{D_0} = \frac{D_2}{D_0} = C W^{-2} \quad (6.7)$$

and is thus recovered by comparing F_{comp} with

$$F = \begin{cases} 3C \left(W + \frac{\Delta W}{2} \right)^{-2} & \text{if } W \leq \frac{\Delta W}{2} \\ C \left(W^2 + \frac{(\Delta W)^2}{3} \right)^{-1} & \text{if } W \geq \frac{\Delta W}{2} \end{cases}. \quad (6.8)$$

It is convenient to use the largest obtainable bandwidth $\Delta W = 100$ or $\Delta X = 100$ for the precise determination of C . For $\Delta W = 100$, only $W \leq 50$ occurs, and therefore F_{comp} is compared with $F = 3C(W + 50)^{-2}$. An additional smoothing \bar{F}_{comp} is achieved by averaging over ten F_{comp} -values. Then C is recovered from $\bar{F}(W) = 3C(W + 45)^{-1}(W + 55)^{-1}$. Typical computer results are presented in Figure 7.

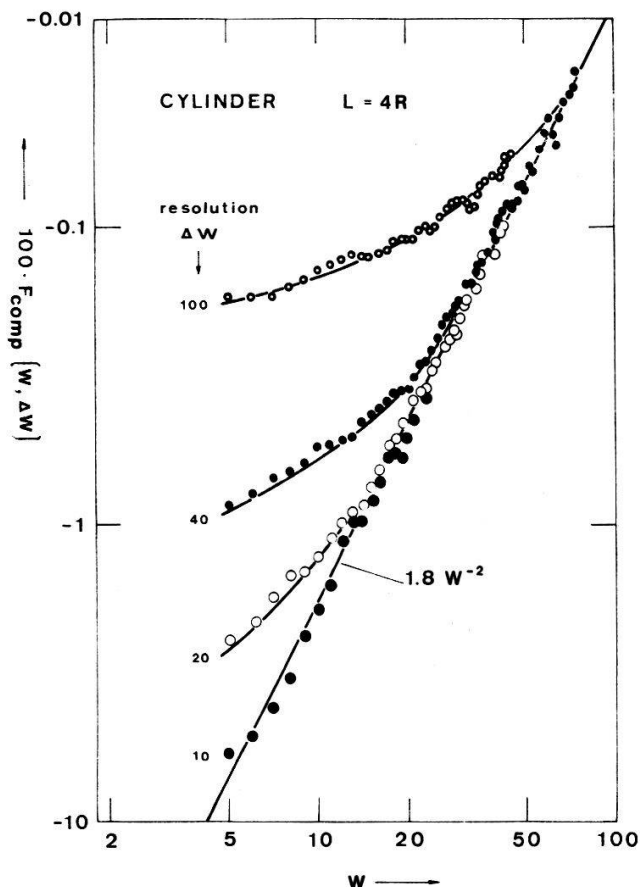


Figure 7

The *second order correction* of the Planck-Weyl mode density D_0 for the *cylindrical cavity* with the length $L = 4R$ in terms of $W = 2L/\lambda$. The computer results $F_{comp} = [D(W, \Delta W) - D_0]/D_0$ are plotted for various spectral resolutions ΔW . The fitted curves correspond to the average correction $D_2/D_0 = -1.8 W^{-2}$.

C. Results for the circular cylinder

1. *Average results.* By the above procedures, we determined the second order correction for a variety of cylindrical cavities with ρ between 0.1 and 10. In terms of $\Omega = 2 V^{1/3}/\lambda$, the results are compiled in Figure 8 and read as follows:

$$D(\Omega) d\Omega = \pi \Omega (1 - C \Omega^{-2}) d\Omega, \quad (6.9)$$

$$C = (0.25 \pm 0.05) (\rho^{1/3} + \rho^{-2/3}). \quad (6.10)$$

The accuracy is discussed in the Appendix A 4. We observe that the cylinder with $\pi R^2 = L^2$ (i.e. $\rho = 2 \pi^{-1/2} = 1.13$) and the cube possess quite similar corrections in terms of Ω with C close to 0.5 in both cases.

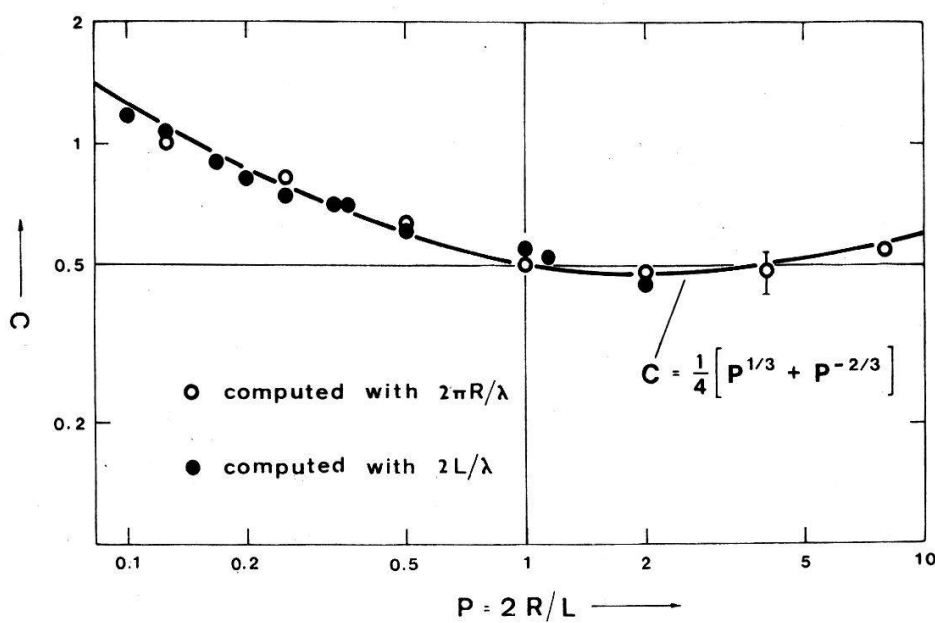


Figure 8

The second order correction of the Planck-Weyl mode density for a variety of *cylindrical resonators*. The coefficient C defined by $D/D_0 = 1 - C \Omega^{-2}$, $\Omega = 2 V^{1/3}/\lambda$, is plotted as a function of the cylinder parameter $\rho = 2 R/L$. The open circles correspond to values obtained by the *X*-programme (6.4), the full black circles to those computed using the *W*-programme (6.5). The fitted curve is $(1/4) (\rho^{1/3} + \rho^{-2/3})$.

In terms of (ν/c) we obtain

$$N = N_0 - \{(1.4 \pm 0.2) L + \pi R\} \left(\frac{\nu}{c}\right) + \bar{\mathcal{O}}(1). \quad (6.11)$$

The coefficient π is obtained from the two-dimensional limit ($L \rightarrow 0$). It is compatible with the corresponding computer value 2.9 ± 0.5 . We point out that (6.11) is purely *conjectural* when considered as an expansion valid in the limit $\nu \rightarrow \infty$. For the present state of the art see the 'Note added in proof' at the end of the paper.

2. *Fluctuations.* For the particular cylinder with $\rho = 2 \pi^{-1/2}$ and volume L^3 we found

$$\bar{\delta}(\nu, \Delta\nu) \approx 0.04 c^2 L^{-2} \nu^{-1} (\Delta\nu)^{-1}. \quad (6.12)$$

The fluctuations are larger for extremely flat or extremely long cylinders, $\phi \gg 1$ or $\phi \ll 1$. An example is shown in Figure 9. For flat cylinders, oscillations similar to those described by (5.22) occur:

$$D_{osc}(\nu) d\nu = \text{const} \frac{R^3}{L} \left(\frac{\nu}{c} \right) \sin \left(4 \pi L \frac{\nu}{c} \right) \frac{d\nu}{c}. \quad (6.13)$$

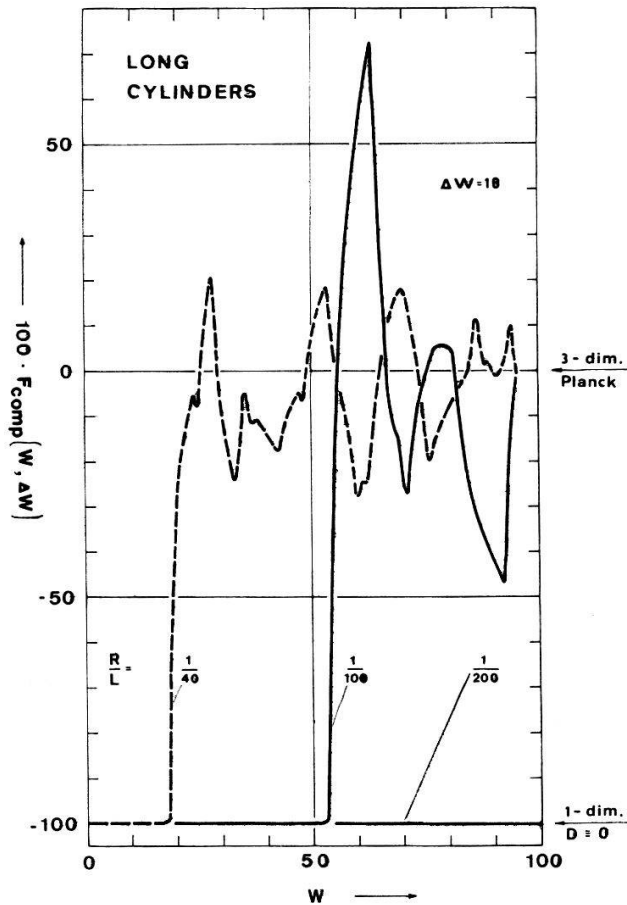


Figure 9

The relative deviations from the Planck-Weyl mode density D_0 for *extremely long circular cylinders* ($L \gg R$). The computer results $F_{comp} = [D(W, \Delta W = 10) - D^3]/D_0$ are plotted. $W = 2 L/\lambda$. For $W \gtrsim L/2R$, we find $D = 0$. This agrees with the cut off [113], $R \leq (j_{11}/2\pi) \approx 0.3\lambda$.

D. Results for sectoral cavities

Let Φ denote the sectoral angle of a cavity defining the shape of a sector out cut of a circular cylinder. For $\Phi = \pi/k$, $k = 1, 2, 3, \dots$, the eigenvalues are easily obtained from (6.1/2) by omitting certain quantum numbers (m, l, n) . For the half-cylinder with $\Phi = \pi$, we find the table

m	n	G_E	G_H	
0	0	0	0	
0	> 0	0	$1 \text{ if } l \geq 2$ $0 \text{ if } l = 1$	
> 0	0	1	0	
> 0	> 0	1	1	

instead of (6.3). For $\Phi = \pi/k$, out of the $m > 0$ only the values $m = k, 2k, 3k, \dots$ survive. For $\Phi \ll \pi$, the only solutions providing low frequency modes are $(0, 1 \geq 2, n > 0)$. Thus, the extremely narrow sector shows a two-dimensional low-frequency mode density.

Computer results combined with limit considerations lead to

$$N = N_0 - \left\{ 0.25(A + \Phi)L + \left(1 + \frac{\Phi}{2}\right)R \right\} \left(\frac{\nu}{c}\right) + \dots \quad (6.15)$$

with the fitted values $A = 2, 3, 5/2$ for $\Phi = \pi, \pi/2, \pi/4$, respectively. In Figure 10, the computer results are compared with (6.15) in terms of $X = 2\pi R/\lambda$. We observe that in terms of Ω , square, circular, and sectoral cylinders possess fairly similar second order corrections.

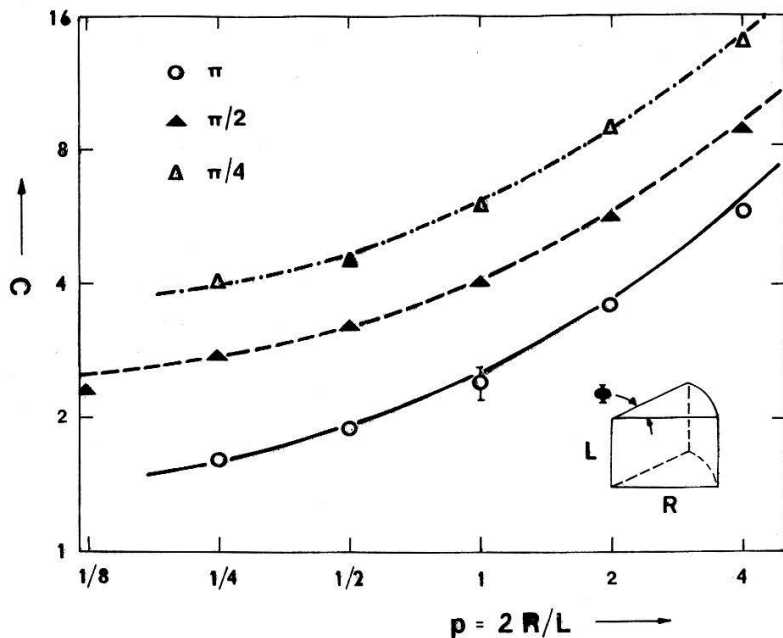


Figure 10

The average second order correction of the Planck-Weyl mode density D_0 for sectoral cavities. The computer results for the constant C defined by $D/D_0 = 1 - C X^{-2}$, $X = 2\pi R/\lambda$, are plotted as a function of $p = 2R/L$ for the sector angles $\Phi = \pi, \pi/2, \pi/4$. The fitted curves $C = (\pi/4\Phi)[A + \Phi + p(\Phi + 2)]$ correspond to the relation (6.15) with $A = 2, 3, 5/2$.

E. Two-dimensional limits

For the full cylinder, as well as for the sectors, we studied the limit $L \rightarrow 0$. According to (3.11) we expect

$$D \rightarrow D^{\text{II}} = D_0^{\text{II}} \left(1 - C \left(\frac{\gamma}{\sigma} \right) \left(\frac{c}{\nu} \right) \right), \quad (6.16)$$

with $C = 1/4\pi = 0.07977 \dots$. For Φ between 2π and $\pi/4$, our X -program produced $0.080 \gtrsim C \gtrsim 0.0785$ in excellent agreement with (6.16). From (6.4) we learn

that for $p \gg 1$ the only low frequency modes are $X_E(m, l, 0) = j_{m,l}$, i.e. we count the 'pure' Bessel zeros. Hence, the above result represents a valuable confirmation of our Bessel program.

7. The Second Order Correction for the Sphere and Spherical Sectors

A. The sphere

The scalar wave potentials for the spherical resonator with radius R are

$$u_E = u_H = j_l(x) P_l^m(\cos \vartheta) e^{im\varphi}, \quad (7.1)$$

[113], [114] where j_l denotes the l -th spherical Bessel function,

$$j_l(x) = x^{-1/2} J_{l+1/2}(x), \quad (7.2)$$

with $x = 2\pi r \nu/c$ and $l = 0, 1, 2, 3, \dots$

(i) With the eigenvalues

$$X = 2\pi R \left(\frac{\nu}{c} \right) = a_{l,s}, a'_{l,s}, \quad (7.3)$$

the functions (7.1) fulfil the *scalar Dirichlet* and *Neumann* problems, respectively. The $a_{l,s}$ and $a'_{l,s}$ are the s -th zeros of $j_l(x)$ and $(d/dx) j_l(x)$, respectively, where $s = 1, 2, 3, \dots$. The degeneracy is

$$g = g' = 2l + 1. \quad (7.4)$$

(ii) The electromagnetic fields derived from (7.1) correspond to the eigenvalues:

$$X_E \approx a'_{l,s}, \quad X_H = a_{l,s}. \quad (7.5)$$

Rigorously, the X_E are the solutions of the equation

$$\left[\frac{d}{dx} (x j_l(x)) \right]_{x=X} = 0 \quad (7.6)$$

and the $a'_{l,s}$ represent an approximation. The field components vanish identically for $l = 0$ [114], and the corresponding resonance frequencies are discarded. Hence

$$G_E = G_H = 2l + 1 \quad \text{if} \quad l > 0, \quad G_E = G_H = 0 \quad \text{if} \quad l = 0. \quad (7.7)$$

The computer results based on (7.5-7) were published in a previous paper [93]. The second order correction to the mode density reads

$$N - N_0 = - (5.3 \pm 1.3) R \left(\frac{\nu}{c} \right). \quad (7.8)$$

The low accuracy is due to the approximation (7.5) as well as to the extremely large fluctuations of the spectrum (see Fig. 1).

The above result is at variance with the positive second term

$$N - N_0 = + \left(\frac{8}{3} \right) R \left(\frac{\nu}{c} \right), \quad (7.9)$$

found by Balian and Bloch [125]. We think that this relation is erroneous because the accidental vanishing of the ($l = 0$) fields has been overlooked. This can be illustrated as follows: Because the sphere has no edges, it seems possible to apply the scalar potential method used in Section 4. The boundary conditions read

$$u_H = 0, \quad \frac{\partial}{\partial n} u_E = 0, \quad (7.10)$$

for $x = X$. Adding up the well-known contributions (3.13) of both the scalar Dirichlet and Neumann problems leads to

$$N - N_0 = 2 \cdot \left(\frac{1}{6\pi} \right) \int_S 2 R^{-1} dS \cdot \left(\frac{\nu}{c} \right) = \left(\frac{8}{3} \right) R \left(\frac{\nu}{c} \right), \quad (7.11)$$

i.e. Balian and Bloch's result. It does not apply to the black-body problem because it corresponds to (7.3/4) rather than to (7.5-7). In particular, the resonances $X_E \approx a'_{0,s}$ and $X_H = a_{0,s}$ belonging to vanishing electromagnetic fields are included. Because of $a_{0,s} \approx \pi s$ and $a'_{0,s} \approx \pi s - \pi/2$, the error in $D(X) dX$ is approximately $2/\pi$. This leads to the crude estimate

$$N - N_0 \approx \left(\frac{8}{3} - 4 \right) R \left(\frac{\nu}{c} \right) < 0, \quad (7.12)$$

i.e. a negative second order term. The remaining discrepancies are supposed to be due to the various approximations.

B. The hemisphere

The eigenvalues are given by (7.5/6), but the degeneracies are $G_E = 1$, $G_H = 1 + 1$ if $l > 0$ and $G_E = G_H = 0$ if $l = 0$. Our previous computer result [93] leads to

$$N - N_0 = - (4.7 \pm 1.3) R \left(\frac{\nu}{c} \right). \quad (7.13)$$

C. The cones

The case of the cones or spherical sectors with half-angle $\theta < \pi/2$ is the most complicated considered so far. The equations

$$P_\varrho^m(\cos\theta) = 0, \quad P_\varrho^{m'}(\cos\theta) = 0, \quad (7.14)$$

for the index ϱ of the Bessel function j_ϱ have to be solved. This requires further approximations [93], and no more than the order of magnitude of the second order coefficient is obtained. For $\theta = \pi/4$, $\pi/6$, and $\pi/12$, we computed

$$N - N_0 = - C R \left(\frac{\varrho}{c} \right), \quad (7.15)$$

with $C \approx 2$, 1, and 0.5.

8. A Comprehensive Conjecture

The average second order correction for (i) the rectangular parallelepiped (5.19), (ii) the circular cylinder (6.11), (iii) the half-cylinder (6.15) with $A = 2$, and (iv) the quarter-cylinder (6.15) with $A = 3$ can be summarized in the following *conjecture*:

$$N - N_0 = - \frac{1}{4} \left(\sum_i l_i + \sum_K m_k \right) \left(\frac{\varrho}{c} \right). \quad (8.1)$$

The l_i indicate the lengths of the *rectangular* edges of the resonator. The m_k are defined as follows:

$$m_k = \int_{S_k} dS_K (R_{k1}^{-1} + R_{k2}^{-1}), \quad (8.2)$$

where S_k denotes the k -th smooth component of the boundary surface with R_{k1} and R_{k2} as principal radii of curvature. Flat faces with $R_1 = R_2 = 0$ yield a zero contribution. Because of the inaccuracy of the numerical results (6.11/15), we must admit an unknown factor close to one (e.g. $3/\pi$) in (8.2). Cavities with non-rectangular edges are not described by (8.1).

For the sphere and the hemisphere, the above conjecture leads to $N - N_0 = - C R(\varrho/c)$ with $C = 2\pi$ and $C = 3\pi/2$, respectively. This is in good agreement with our computer results (7.8/13). For the cones studied in 7.C, the conjecture yields $C = 2.8$, 1.9, and 0.9 compatible with the fairly inaccurate computer values (7.15). We mention that for extremely narrow cones ($\theta \gg \pi/2$), the conjecture leads to

$$N - N_0 = - \frac{\pi}{2} R \sin \theta \cdot \left(\frac{\varrho}{c} \right). \quad (8.3)$$

In the following sections we make use of the quantity A with the dimension of a length. In terms of A , the corrected mode density reads

$$D(\varrho) d\varrho = \left(D_0(\varrho) - \frac{A}{c} \right) d\varrho = D_0(\varrho) \left(1 - \frac{A}{8\pi V} \left(\frac{c}{\varrho} \right)^2 \right) d\varrho. \quad (8.4)$$

According to the results obtained in the preceding sections, A depends on the linear dimensions of the resonator:

$$\left. \begin{array}{ll}
 \text{cube} & A = 3L \\
 \text{parallelepiped} & A = L_1 + L_2 + L_3 \\
 \text{circular cylinder} & A = (1.4 \pm 0.2)L + \pi R \\
 \text{half-cylinder} & A = (1.3 \pm 0.2)L + \left(1 + \frac{\pi}{2}\right)R \\
 \text{quarter-cylinder} & A = (1.1 \pm 0.2)L + \left(1 + \frac{\pi}{4}\right)R \\
 \text{eighth-cylinder} & A = (0.8 \pm 0.1)L + \left(1 + \frac{\pi}{8}\right)R \\
 \text{sphere} & A \approx 6R \\
 \text{hemisphere} & A \approx 5R \\
 \text{cones } (15^\circ \dots 45^\circ) & A = (0.5 \dots 3)R
 \end{array} \right\} \quad (8.5)$$

9. The Correction of Wien's Displacement Law

With $h\nu/kT = x$, the equation for x_{max} reads

$$\frac{d}{dx} \left\{ \frac{x^3 - Bx}{e^x - 1} \right\} = 0, \quad x > 0, \quad B = \frac{A}{8\pi V} \left(\frac{h c}{k T} \right)^2. \quad (9.1)$$

This leads to the transcendental equation

$$\frac{e^x - 1}{e^x} = \frac{x^3 - Bx}{3x^2 - B}. \quad (9.2)$$

The quantity x_{max} is meaningful only if c/ν is well below the cut-off wavelength of the cavity, i.e. for sufficiently large temperatures and volumes. Hence we assume $B \ll 1$, which leads to

$$x - x_0 \approx \left(\frac{2}{3} \right) B x_0^{-1}, \quad x_0 = 2.822 = x \quad (B = 0), \quad (9.3)$$

whence

$$\frac{h\nu_{max}}{kT} - 2.822 \approx 0.01 \frac{A}{V} \left(\frac{h c}{k T} \right)^2. \quad (9.4)$$

E.g. for the cube with edge length L , the right side of (9.4) reads $(0.24/T[K] L[cm])^2$.

10. Refinements of the Stefan-Boltzmann Formula

A. An Abelian and a Tauberian theorem for the Bose-Einstein summation

The total radiation energy $E(T)$ is usually computed by formal integration of the asymptotic frequency density multiplied with the Bose-Einstein factor. Actually, this integration is justified by the following *Abelian theorem*:

Let $D(x)$ be the eigenvalue density of a regular elliptic boundary value problem with $D(x) \sim a x^n$ if $x \rightarrow \infty$ for some real $n > -1$. Then, for $t \rightarrow \infty$,

$$\int_0^\infty \frac{x}{e^{x/t} - 1} D(x) dx \sim a \Gamma(n+2) \zeta(n+2) t^{n+2}. \quad (10.1)$$

Since Case and Chiu [127] determined the second order correction $E_2(T)$ (3.10) for the total energy of the cube shaped resonator, the converse of the above theorem has gained physical relevance. We should like to derive the asymptotic behaviour of $D_2(v)$ from that of $E_2(T)$. This implication is not valid, unless $D_2(v)$ is subjected to additional conditions. Looking for these conditions, we found the *Tauberian theorem*:

If

$$\int_0^\infty \frac{x}{e^{x/t} - 1} D(x) dx \sim A t^m,$$

for $t \rightarrow \infty$ for some real $m > 1$, and if $x^{2-m} D(x)$ is bounded and slowly decreasing, then

$$D(x) \sim \frac{A}{\Gamma(m) \zeta(m)} x^{m-2} \quad \text{for } x \rightarrow \infty. \quad (10.2)$$

With $n = 2$, theorem (10.1) constitutes a rigorous proof of the Stefan-Boltzmann formula and constant, based on Weyl's theorem [131], [132]. With $m = 2$, and Case and Chiu's term $E_2(T)$, theorem (10.2) yields $D - D_0 = D_2 \sim -3 L/c$ if $v \rightarrow \infty$. This is in excellent agreement with the result found in Section 5. The proofs of the above theorems will be published elsewhere [150]. They are based on Wiener's first Tauberian theorem [151] and on the non-vanishing of the zeta function $\zeta(s)$ for arguments with $\text{Re}(s) > 1$ [152].

B. The second order correction

The refinements of the mode density lead to the corresponding expansion of the total radiation energy, viz. $E(T) = E_0(T) + E_1(T) + E_2(T) + \dots$, where $E_0(T) = (4 \sigma/c) V T^4$ represents the Stefan-Boltzmann formula (1.9). The first order or surface term $E_1(T)$ vanishes. The first non-vanishing correction is

$$E_2(T) = -\frac{\pi^2}{6} \frac{A}{h c} (k T)^2, \quad (10.3)$$

with Λ given in the Table (8.5). E.g. for the circular cylinder with $\rho = 2 R/L$ this leads to

$$\frac{E_2}{E_0} \approx -(\rho + 1) (10 R [\text{cm}] T [\text{K}])^{-2}. \quad (10.4)$$

These results are meaningful only if T is large enough to populate modes well above the cut-off frequency of the resonator.

C. The measurement of the Stefan-Boltzmann constant

Many experimental determinations of the Stefan-Boltzmann constant have been reported since 1915. A survey is given in the Ref. [22] and [153]. Only the most recent measurements made by Blevin and Brown [153] at the freezing point of gold produced a result consistent with the theoretical value. Without exception, all the prior experimental values were higher than σ_{theor} . The differences range between 0.3% and 2.2%. The above refinements of the Stefan-Boltzmann formula are *not* responsible for these discrepancies. They lead to

$$\sigma_{\text{exp}} = \frac{I}{T^4} = \varrho_{\text{theor}} - \frac{\sigma'}{T^2} < \varrho_{\text{theor}}. \quad (10.5)$$

Besides, the correction is extremely small for high temperatures. For the black-body used by Blevin and Brown [153] we find the insignificant correction $E_2/E_0 \approx -3 \cdot 10^{-9}$. In the case of Kendall's low-temperature measurements we estimate -10^{-7} for the radiometer and $-2 \cdot 10^{-5}$ for the large 77 K test cavity.

D. Higher order corrections

(i) The *third* order correction $N_3(\nu) = 1/2$ valid for the *parallelepiped* formally corresponds to a single resonance of arbitrarily low frequency with the weight 1/2. Thus the contribution to the total radiation energy is

$$E_3(T) = \lim_{\hbar\nu/kT \rightarrow 0} \frac{1}{2} \left[\frac{\hbar\nu}{e^{\hbar\nu/kT} - 1} \right] = \frac{1}{2} k T. \quad (10.6)$$

This agrees with Case and Chiu's result for the cube [127].

(ii) In the case of the *extremely flat square prism* ($L/L_3 = \rho \gg 1$), the integration of the oscillatory term D_4 (5.22) yields

$$E_4 \approx \frac{30}{\pi^4} \rho E_0 y^{-1} \int_0^\infty \frac{x^2 \sin xy}{e^x - 1} dx, \quad \left. \right\} \quad (10.7)$$

$$y = \frac{2 k T L_3}{\hbar c}.$$

The integral in (10.7) is related to the Langevin function [154]

$$L(x) = \coth x - \frac{1}{x}, \quad (10.8)$$

as well as to the generalized Riemannian function [155]

$$\zeta(s, a) = \sum_{n=0}^{\infty} (a + n)^{-s} = \frac{1}{\Gamma(s)} \int_0^{\infty} \frac{x^{s-1} e^{-ax}}{1 - e^{-x}} dx \quad (10.9)$$

viz.

$$\int_0^{\infty} = -\frac{\pi}{2} \frac{d^2}{dy^2} L(\pi y) \quad \text{or} \quad (10.10)$$

$$\int_0^{\infty} = -2 \operatorname{Im}[\zeta(3, 1 + iy)]. \quad (10.11)$$

The evaluation of (10.11) yields

$$E_4 = 2 \not p E_0 C_E''(y), \quad (10.12)$$

with

$$C_E''(y) = \frac{30}{\pi^4} \sum_{m=1}^{\infty} \frac{3m^2 - y^2}{(m^2 + y^2)^3}. \quad (10.13)$$

A plot of $C_E''(y)$ for y between 0 and 2 is found on p. 296 in Ref. [103]. The above relations enable us to describe the asymptotic behaviour of E_4 :

$$y \gg 1 \quad \text{i.e.} \quad L_3 T \gg 0.1 \text{ cm K}.$$

From (10.10) we obtain

$$\int_0^{\infty} \rightarrow y^{-3} - 4\pi e^{-2\pi y} \quad \text{for} \quad y \rightarrow \infty \quad (10.14)$$

and therefore

$$E_4 \approx \frac{\hbar c}{\pi} \frac{L^3}{L_3^4} \left\{ \frac{1}{8\pi} - \left(\frac{2kT L_3}{\hbar c} \right)^3 e^{-4\pi k T L_3 / \hbar c} \right\}. \quad (10.15)$$

$$y \ll 1 \quad \text{i.e.} \quad L_3 T \ll 0.1 \text{ cm K}.$$

In the limit $y \rightarrow 0$, the function (10.13) reads $C_E''(0) = 1$. Hence

$$E_4 = 2 \not p E_0 \sim T^4. \quad (10.16)$$

As a consequence, the only significant term in the low temperature expansion would be E_3 leading to

$$E(T) \rightarrow \frac{1}{2} k T \quad \text{for} \quad L_3 T \rightarrow 0. \quad (10.17)$$

in formal agreement with a conjecture by Case and Chiu [127]. But (10.17) is obtained by inconsistently applying the $L_3 T \rightarrow 0$ limit to the mode density (5.22) valid for $L_3 \gg c/2\nu$ and thus does not provide the correct answer. Furthermore (10.17) is at variance with the third principle of thermodynamics. The correct $T \rightarrow 0$ behaviour reads $\exp(-\text{const}/T)$ and is studied in a forthcoming paper [156].

E. Thermodynamic properties of the radiation field

The total radiation energy of the photon gas with the second order correction can be written as

$$E(V, T) = a_0 V T^4 - a_2 V^{1/3} T^2, \quad (10.18)$$

where

$$a_2 = \frac{\pi^2}{6} \frac{k^2}{h c} \Lambda V^{-1/3}. \quad (10.19)$$

The dimensionless parameter $\Lambda V^{-1/3}$ depends on the shape, but not on the volume, of the cavity. From (10.18), further thermodynamic properties are easily derived [93]:

$$\text{entropy} \quad S = S_0 - 2 a_2 V^{1/3} T, \quad (10.20)$$

$$\text{free energy} \quad F = F_0 - a_2 V^{1/3} T^2, \quad (10.21)$$

$$\text{specific heat} \quad C_v = C_{v,0} - 2 a_2 V^{1/3} T, \quad (10.22)$$

$$\text{radiation pressure} \quad p = p_0 - \left(\frac{1}{3}\right) a_2 V^{-2/3} T^2, \quad (10.23)$$

with $F_0 = -E_0/3$, $S_0 = 4 E_0/3 T$, $C_{v,0} = 4 E_0/T$, $p_0 = E_0/3 V$. We mention that in the high-temperature limit the complete expansion is of the form

$$E(V, T) \sim a_0 V T^4 - a_2 V^{1/3} T^2 + a_3 T + a_4 V^{-1/3} + \dots \quad (10.24)$$

The relation $p V = E/3$ remains correct for finite cavities. For the photon gas this relation seems to play the role of the Landsberg condition $p V = 2 E/3$ valid for *non-relativistic* perfect gases [144].

11. Refinements of the Temporal Autocorrelation

The theory of the *complex coherence function* or *second order correlation tensor* (1.11) of the electric and magnetic fields has to be modified for finite cavities. We restrict our considerations to the *first order* correction of the *temporal auto-correlation* ($\mathbf{r} = \mathbf{r}_2 - \mathbf{r}_1 = 0$, $i = j$). In the infinite space approximation, these functions are [100], [101]:

$$\mathcal{E}_{ii,0} = \mathcal{E}_0 = \mathcal{H}_0 = \mathcal{H}_{ii,0} = \frac{16 (k T)^4}{\pi (\hbar c)^3} \zeta(4, 1 + i \tau), \quad \tau = \left(\frac{k T}{\hbar}\right) t. \quad (11.1)$$

The generalized zeta function is defined by (10.9).

Let us consider the modes with non-vanishing E_3 - and H_3 -components, respectively. In the relation (1.12) we substitute $D_0/2$ by D_E (4.11) and D_H (4.12), respectively. We obtain

$$\mathcal{E}_{33} - \mathcal{E}_0 = -(\mathcal{H}_{33} - \mathcal{H}_0) = \frac{4 (k T)^3}{3 (\hbar c)^2} \left(\frac{S_{\perp} - S_{\parallel}}{V}\right) \zeta(3, 1 + i \tau). \quad (11.2)$$

Details of the calculation are found in [93]. We observe that the refined components \mathcal{E}_{11} , \mathcal{E}_{22} , and \mathcal{E}_{33} are in general different from each other, as well as $\mathcal{H}_{ii} \neq \mathcal{E}_{ii}$. As an example we mention the parallelepiped:

$$\mathcal{E}_{ii} - \mathcal{E}_0 = \frac{8 (k T)^3}{3 (\hbar c)^2} \left\{ L_i^{-1} - (L_{i+1}^{-1} + L_{i+2}^{-1}) \right\} \zeta(3, 1 + i \tau). \quad (11.3)$$

The indices of the edge lengths L_i are counted modulo 3, and $L_3 \parallel E_3$. The \mathcal{E}_{ii} are equal in the case of the cube.

12. The Correction of the Lamb-Shift

Using the result (8.4), we substitute D_0 in the relation (1.14) by $D_0 - \Lambda/c$. Because of $\nu_1 \ll \nu_2$, we find the relative deviation

$$\delta E = \frac{(\Delta E - (\Delta E)_0)}{(\Delta E)_0} = - \frac{c^2}{16 \pi} \frac{\Lambda}{V} \nu_1^{-2} \left(\frac{(\log \nu_2)}{\nu_1} \right)^{-1}. \quad (12.2)$$

With $\log(\nu_2/\nu_1) = 7.36$ and $\nu_1 = 2.9 R y c \approx 10^{13} \text{ sec}^{-1}$ [106], we calculate

$$\delta E \approx -2.7 \cdot 10^{-9} \frac{\Lambda [\text{cm}]}{V[\text{cm}^3]}, \quad (12.2)$$

i.e. an irrelevant correction. We observe that δE is so small because only wavelengths $\lambda \gg c/\nu_1 \approx 30 \mu\text{m}$ are considered. Furthermore, the above result has the character of an average taken over the cavity volume. More important deviations probably occur for atoms at positions very close to the ideally reflecting resonator wall.

Appendix

A 1. An Illustration of Carleman's Method

As an illustration of the methods mentioned in Section 3.B we prove Weyl's theorem by a Carleman procedure. Consider the heat diffusion equation

$$\nabla^2 u - \frac{\partial}{\partial t} u = 0. \quad (A.1)$$

The Green function for (A.1) is related to the eigenvalues K_n and the eigenfunctions u_n belonging to the wave equation with Dirichlet or Neumann boundary conditions by

$$f_t(\mathbf{x}, \mathbf{y}) = \sum_n u_n(\mathbf{x}) e^{-K_n t} u_n(\mathbf{y}). \quad (A.2)$$

The integral

$$F(t) = \int_V d^3x f_t(x, x) = \sum_n e^{-K_n^2 t}, \quad (A.3)$$

is the Laplace transform of the eigenvalue density. In the case of Weyl's limit $V \rightarrow \infty$ we may disregard the boundary conditions and use the infinite-space Green function

$$f_{t,0}(x, y) = (4 \pi t)^{-3/2} e^{-|x-y|/4t}. \quad (A.4)$$

Thus we find

$$F(t) \sim F_0(t) = V(4 \pi t)^{-3/2} \quad (A.5)$$

if $t \rightarrow +0$. Here, the intuitive physical argument is that short diffusion times lead to the infinite space approximation [135]. From (A.3) and (A.5) we conclude

$$\int_0^\infty e^{-K^2 t} dN(K^2) \sim V(4 \pi t)^{-3/2}, \quad (A.6)$$

if $t \rightarrow +0$. Applying the Tauberian theorem due to Hardy, Littlewood, and Karamata [140] we obtain

$$N(K^2) \sim \frac{V}{6 \pi^2} (K^2)^{3/2}, \quad (A.7)$$

for $K \rightarrow \infty$. In the infinite-space limit, N_0 (electromagnetic) is equal to $2 N_0$ (scalar), and thus we find

$$N \sim \frac{V}{3 \pi^2} K^3 = \frac{8 \pi}{3} V \left(\frac{v}{c} \right)^3, \quad (A.8)$$

valid for $V \rightarrow \infty$ or $(v/c) \rightarrow \infty$.

A 2. Lattice-Point Problem Connections

A. Definitions

For a cube shaped domain with edge length L , the squared reduced eigenfrequencies of the wave equation can be written as sums of three squared integers,

$$Q = W^2 = \left(\frac{K L}{\pi} \right)^2 = n_1^2 + n_2^2 + n_3^2, \quad (A.9)$$

where the weights $G(n_1, n_2, n_3)$ depend on the physical nature of the problem and on the type of boundary conditions imposed. Consequently, the number $N(Q)$ of *electro-*

magnetic modes of a lossless cube shaped cavity with a reduced frequency not exceeding $Q^{1/2}$ can be represented as

$$N(Q) = \frac{1}{4} F_3(Q) - \frac{3}{2} Q^{1/2} + \frac{1}{2}, \quad (\text{A.10})$$

where $F_3(Q)$ is the number of lattice points (n_1, n_2, n_3) inside a sphere with the radius $Q^{1/2}$. Precise definitions of N and F_3 are given in Section 5.A. In the *two-dimensional limit of the above electromagnetic problem* we have a square shaped domain, and the squared eigenvalues are

$$Q = n_1^2 + n_2^2, \quad (\text{A.11})$$

with $n_i > 0$ and $G(n_1, n_2, n_3) = 1$. This identical with the two-dimensional Dirichlet problem (the ‘square shaped membrane’). Here we find the relation

$$N^{\text{II}}(Q) = \frac{1}{4} F_2(Q) - Q^{1/2} + \frac{1}{4}, \quad (\text{A.12})$$

where $F_2(Q)$ denotes the number of lattice points inside a circle of the radius $Q^{1/2}$.

For convenience we mention the *three-dimensional Dirichlet problem*, where (A.9) is valid with the additional requirement $n_i > 0$ for any i . The connection with the functions F_2 and F_3 is as follows:

$$N^{\text{III}}(Q) = \frac{1}{8} F_3(Q) - \frac{3}{8} F_2(Q) + \frac{3}{4} Q^{1/2} - \frac{1}{8}. \quad (\text{A.13})$$

$F_\mu(Q)$ can be written as a sum of the arithmetic functions $r_\mu(Q)$, which denote the number of representations of the integer Q as a sum of μ squares. E.g. $r_2(Q)$ is the number of lattice points touching the circumference of the circle with the radius $Q^{1/2}$. I.e., we count representations as distinct even when they differ only in respect of the sign and the order of the n_i .

B. The functions $r_2(Q)$ and $F_2(Q)$

From elementary number theory we recall the following results [A1] valid for $Q > 1$:

$$r_2(Q) = 8 \quad \text{if} \quad Q = 4m + 1 = \text{prime}, \quad (\text{A.14})$$

$$r_2(Q) = 0 \quad \text{if} \quad Q = 4m + 3 = \text{prime}, \quad (\text{A.15})$$

$$r_2(Q) = 4(d_1(Q) - d_3(Q)) \quad \text{with} \quad Q = 2^\alpha \prod p^r \prod q^s, \quad (\text{A.16})$$

where p and q are primes $4m + 1$ and $4m + 3$ respectively, and $d_1(Q)$ and $d_3(Q)$ are the numbers of prime divisors of Q of the form $4m + 1$ and $4m + 3$, respectively. The asymptotic behaviour $F_2 \sim \pi Q$ was known already to Gauss [A2]. The refined asymptotic relation

$$F_2(Q) = \pi Q + \mathcal{O}(Q^{\theta + \epsilon}), \quad (\text{A.17})$$

valid for arbitrary $\varepsilon > 0$ has been the starting point of a great deal of modern work. The aim is the determination of the real number θ . Geometrical arguments show that $\theta \leq 1/2$ [A2]. We list the refinements of this estimate:

$\theta \leq \frac{1}{3}$	Sierpiński	1906 [A3],	
$\theta \geq \frac{1}{4}$	Landau and Hardy	1915 [A4], [A5],	
$\theta < \frac{1}{3}$	Van der Corput	1923 [A6],	
$\theta < \frac{37}{112}$	Littlewood and Walfisz	1924 [A7],	(A.18)
$\theta \leq \frac{27}{82}$	Nieland	1928 [A8],	
$\theta \leq \frac{17}{53}$	Vinogradov	1932 [A10],	
$\theta \leq \frac{15}{46}$	Titchmarsh	1935 [A9],	
$\theta \leq \frac{12}{37}$	Yin	1962 [A11].	

As a consequence, the asymptotic expansion for the eigenfrequencies of the square drum reads

$$N^{\text{II}}(Q) = \frac{\pi}{4} Q - Q^{1/2} + \mathcal{O}(Q^\theta), \quad (\text{A.19})$$

with $0.32 \gtrsim \theta \geq 0.25$.

According to Landau and Hardy, θ cannot be smaller than $1/4$. A further refinement of (A.17) is achieved only if the averaged asymptotic behaviour $\tilde{\mathcal{O}}$ instead of \mathcal{O} is investigated. Brownell [126] was able to show that

$$F_2(Q) = \pi Q + \tilde{\mathcal{O}}(Q^{-r}), \quad (\text{A.20})$$

where r is an arbitrary positive real number. $\tilde{\mathcal{O}}$ denotes the *log Gaussian average*. A shortened version of the definition of $\tilde{\mathcal{O}}$ reads: We define $f(y) = \tilde{\mathcal{O}}(y^{-r})$ for $r > 0$ over $y > b > 0$ if for every $\varrho > 0$ there exists some $M_\varrho < \infty$ so that

$$\left| \int_b^\infty \exp \left[-\frac{1}{2} \varrho^2 \ln \left(\frac{v}{y} \right) \right] df(y) \right| \leq M_\varrho v^{-r}, \quad (\text{A.21})$$

over $v \geq e$.

As a consequence of (A.20), Brownell obtains

$$N^{\text{II}}(Q) = \frac{\pi}{4} Q - Q^{1/2} + \frac{1}{4} + \tilde{\mathcal{O}}(Q^{-r}) . \quad (\text{A.22})$$

C. The functions $r_3(Q)$ and $F_3(Q)$

In the three-dimensional case the results are less complete [A1]:

$$r_3(Q) = 0 \quad \text{if} \quad Q = 4^k(8m + 7) , \quad k, m = 0, 1, 2, \dots , \quad (\text{A.23})$$

$$r_3(Q) > 0 \quad \text{if} \quad Q \neq 4^k(8m + 7) . \quad (\text{A.24})$$

According to Eisenstein [A12]

$$r_3(4m + 1) = 24 \sum_{l=1}^m \left(\frac{l}{4m+1} \right) \text{ for prime } 4m + 1 , \quad (\text{A.25})$$

$$r_3(4m + 3) = 8 \sum_{l=1}^m \left(\frac{l}{4m+3} \right) \text{ for prime } 4m + 3 , \quad (\text{A.26})$$

where (l/n) is the *Legendre-Jacobi symbol* [A1]. The above relations are useful for controlling the computation of $N(Q)$.

For comparison, we mention the simple and complete results for the case $\mu = 4$ [A1]:

$$r_4(Q) > 0 \quad \text{for any } Q , \quad (\text{A.27})$$

$$r_4(Q) = 8 \text{ times the sum of the divisors of } Q \text{ which are not multiples of 4} . \quad (\text{A.28})$$

Obviously, the *odd* dimension 3 is a rather complicated case compared to $\mu = 2$ and 4.

Geometrical arguments show that

$$F_3(Q) = \frac{4\pi}{3} Q^{3/2} + \mathcal{O}(Q) . \quad (\text{A.29})$$

Landau [A13] obtained

$$F^3(Q) = \frac{4\pi}{3} Q^{3/2} + \mathcal{O}\left(Q \frac{3}{4} + \varepsilon\right) , \quad (\text{A.30})$$

improving the earlier refinement $5/6 + \varepsilon$ [A14]. Todays best estimate with the exponent $19/28$ has been found by Vinogradov as reported in [147]. Brownell [126] found the averaged estimate

$$F^3(Q) = \frac{4\pi}{3} Q^{3/2} + \tilde{\mathcal{O}}(Q^{-r}) . \quad (\text{A.31})$$

As a consequence of (A.10), (A.13), (A.20) and (A.31), the following *average* results are valid:

$$N(Q) = \frac{\pi}{3} Q^{3/2} - \frac{3}{2} Q^{1/2} + \frac{1}{2} + \tilde{\mathcal{O}}(Q^{-r}) , \quad (\text{A.32})$$

for the electromagnetic problem, and

$$N^{III}(Q) = \frac{\pi}{6} Q^{3/2} - \frac{3}{8} \pi Q + \frac{3}{4} Q^{1/2} - \frac{1}{8} + \tilde{\theta}(Q^{-r}), \quad (A.33)$$

for the three-dimensional scalar Dirichlet problem.

It can be shown [A15] that 1 out of 6 numbers has, in the average, the form (A.23). Thus the average level distance is $\Delta Q = \Delta(W^2) = 6/5$ and hence $\Delta W = (6/5)/2 W$. As a consequence, the mean degeneracy of an eigenvalue W is

$$\bar{G}(W) = \frac{3}{5W} \cdot \frac{d}{dW} N(W) \approx \frac{3}{5} \pi W. \quad (A.34)$$

D. The numbers $(Q, Q = n_1^2 + n_2^2 + n_3^2 \rightarrow n_1 \cdot n_2 \cdot n_3 = 0)$

We mentioned above (A.13) that in the case of the scalar Dirichlet problem only the lattice points (n_1, n_2, n_3) with $n_1 \cdot n_2 \cdot n_3 > 0$ are counted. Thus, those numbers Q which can be represented as a sum of three squares if and only at least one of the n_i is zero, have to be discarded. Hilf [148] studied this particular set

$$(Q, Q = n_1^2 + n_2^2 + n_3^2 \rightarrow n_1 \cdot n_2 \cdot n_3 = 0) \quad (A.35)$$

and found the representation

$$Q = 4^n r_i, \quad (A.36)$$

where $n = 0, 1, 2, \dots, i = 0, 1, \dots, 10$, and where the numbers r_0, \dots, r_{10} are

$$0, 1, 2, 5, 10, 13, 25, 37, 58, 85, 130. \quad (A.37)$$

We extended Hilf's computer investigations and confirmed that (A.36) is valid for $Q < 40000$. In particular, no further 'basic number' r_i beyond (A.37) is needed. For $32 < Q < 40000$ we also found the new relations [A16]

$$\left. \begin{aligned} Q_{10m+a} &= 4^{m-1} Q_{10+a}, \\ Q_{10m'+b} &= 4^{m'-2} Q_{20+b}. \end{aligned} \right\} \quad (A.38)$$

with $a = 3, 4, \dots, 9$, $m \geq 1$, and $b = 0, 1, 2$, $m' \geq 2$. Here, (Q_j) is an ordered set with $Q_1 = 0$. The basic numbers for (A.38) are Q_{13}, \dots, Q_{22} and read

$$37, 40, 52, 58, 64, 80, 85, 100, 128, 130. \quad (A.39)$$

A 3. Electromagnetic Modes in Cylindrical Cavities

For the lossless pill-box cavity with the length L and the radius R the scalar wave potentials are [113]

$$\left. \begin{aligned} u_E &= A e^{im\varphi} J_m(\eta r) \cos \beta z, \\ u_H &= A e^{im\varphi} J_m(\eta' r) \sin \beta z, \end{aligned} \right\} \quad (A.40)$$

with J_m = Bessel function of the order m , $\eta = j_{m,l}/R$, $\eta' = j'_{m,l}/R$, $\beta = n\pi/L$, where $j_{m,l}$ and $j'_{m,l}$ are the l -th zeros of J_m and its derivative J'_m , n = integer, and A is a constant. The resonance frequencies are

$$\left(\frac{\omega}{c}\right)^2 = \begin{cases} \eta^2 + \beta^2 \\ \eta'^2 + \beta^2 \end{cases}, \quad (A.41)$$

Replacing $e^{im\varphi}$ in (A.40) by $\cos m\varphi$, the field components described in Ref. [113], p. 234 and 235, are obtained.

For the computation of the eigenvalue density, a careful discussion of the allowed 'quantum numbers' m, l, n and their respective degeneracies is indispensable. If $m > 0$, the factor $e^{im\varphi}$ in (A.40) is responsible for two independent solutions ($\sin m\varphi, \cos m\varphi$). For the *E-type resonances* we thus find the weight $G_E = 2$, whereas $G_E = 1$ for $m = 0$. Because of $j_{m,l} > 0$ for $l = 1, 2, 3, \dots$, any of these l may occur. Similarly, n may take the values $n = 0, 1, 2, 3, \dots$. Negative n are allowed, but do not lead to additional independent solutions and therefore are redundant. For $m = 0$ and $n = 0$, we still have the non-vanishing field components E_z and H_φ . This is quite different from the behaviour of the *H-type resonances*: All the field components vanish if $n = 0$, i.e. $\beta = 0$, for arbitrary m, l . Hence, $G_H(m, l, 0) = 0$. Furthermore, zero amplitudes are obtained if $m = 0$ and $l = 1$ because of $j'_{0,1} = 0$, i.e. $\eta' = 0$ and $(d/dr) J_m(\eta' r) = 0$. Hence, $G_H(0, 1, n) = 0$. The weights are summarized in the table in Section 6.A. We point out that for all the non-vanishing solutions, $E_z \neq 0, H_z = 0$ and $E_z = 0, H_z \neq 0$ are valid for the *E*- and *H*-type, respectively. Thus the density of the modes with non-vanishing E_z is identical with the *E*-type desnity D_E , an the analogous statement holds for H_z . This remark is essential for the calculation of the (z, z) -component of the coherence tensor in Section 11.

For *sectoral cavities* with the angle Φ , a possible choice for the additional boundary conditions is

$$\left. \begin{array}{l} E_z = E_r = 0 \\ H_\varphi = 0 \end{array} \right\} \text{at } \varphi = 0, \Phi. \quad (A.42)$$

For $\Phi = \pi$, e.g., this leads to the following restrictions:

E-type: Only the $(\sin m\varphi)$ solutions fulfil (A.42). Thus $G_E = 1$ for $m > 0$ and $G_E = 0$ for $m = 0$.

H-type: Only the $(\cos m\varphi)$ solutions are compatible with (A.42). Hence $G_H = 1$ for $m, n > 0$. If $m = 0$, and $n > 0$, the components E_r, E_z , and H_φ vanish identically for arbitrary φ , and therefore obey (A.42) for any Φ .

The resulting table of weights is given in Section 6.D.

A 4. The Computation of the Zeros of the Bessel Functions

A. Olver's Expansions

Our study of the circular-cylinder-shaped cavity requires the knowledge of all the zeros

$$j_{n,s}, \quad j'_{n,s} \lesssim 100, \quad (A.43)$$

of the Bessel functions J_n and J'_n . The notation (n, s) is now introduced instead of the (m, l) found in technical textbooks [113].

The notation (n, s) with $n = 0, 1, 2, \dots$, and $s = 1, 2, \dots$, is used in the mathematical literature [A17]–[A21]. In order to determine the second order correction of the mode density, an accuracy of 0.001 is adequate. This means 4 to 6 significant figures. Because of

$$j_{n,1}, \quad j'_{n,1} \approx n, \quad (A.44)$$

the range of the well-known tables [A17], [A18] is not sufficient, as it is restricted to $n \leq 20$. The simple McMahon expansions [A22]

$$\left. \begin{aligned} j_{n,s} &\sim \left(\frac{n}{2} - s - \frac{1}{4} \right) \pi, \\ j'_{n,s} &\sim \left(\frac{n}{2} - s - \frac{3}{4} \right) \pi. \end{aligned} \right\} \quad (A.45)$$

valid for $s \gg n \gg 1$ are of unsufficient accuracy and limited in range. For these reasons, we calculated the required 10^4 zeros with the help of a computer program based on *Olver's asymptotic expansions*.

The results of Olver's theory [A19], [A20] are as follows:

$$J_n(nz) \sim \left(\frac{4\zeta}{1-z^2} \right)^{1/4} \left[\frac{Ai(n^{2/3}\zeta)}{n^{1/3}} \sum_{s=0}^{\infty} \frac{A_s(\zeta)}{n^{2s}} + \frac{Ai'(n^{2/3}\zeta)}{n^{5/3}} \sum_{s=0}^{\infty} \frac{B_s(\zeta)}{n^{2s}} \right], \quad (A.46)$$

as $n \rightarrow \infty$. Here, ζ is defined as

$$\frac{2}{3} \zeta^{3/2} = \log \frac{1 + (1 - z^2)^{1/2}}{z} - (1 - z^2)^{1/2}. \quad (A.47)$$

Ai denotes the Airy function. The expansion coefficients A_s and B_s are determined by recurrence relations. The above expansion is uniformly valid with respect to the complex variable z .

From (A.46), Olver obtains rapidly converging expansions for the zeros:

$$j_{n,s} \sim nz + n^{-1}p_1 + n^{-3}p_2 + \dots, \quad (A.48)$$

$$j'_{n,s} \sim nz + n^{-1}q_1 + n^{-3}q_2 + \dots \quad (A.49)$$

with $z = z(\zeta)$ according to (A.47). z , the p_i , the q_i are tabulated as functions of ζ for $-\zeta \leq 7.5$ [A18]. For (A.48),

$$\zeta = n^{-2/3} a_s \quad (A.50)$$

whereas for (A.49)

$$\zeta = n^{-2/3} a'_s. \quad (A.51)$$

Here, a_s and a'_s are the s -th zeros of the Airy function and its derivative,

$$Ai(a_s) = 0, \quad Ai'(a'_s) = 0. \quad (A.52)$$

These zeros are easily calculated with the aid of the asymptotic formulae [A18]

$$a_s \sim -\lambda^{2/3} \left(1 + \frac{5}{48} \lambda^{-2} + \dots \right) \quad \lambda = \frac{3\pi}{8} (4s-1), \quad (\text{A.53})$$

$$a'_s \sim -\mu^{2/3} \left(1 - \frac{7}{48} \mu^{-2} + \dots \right) \quad \mu = \frac{3\pi}{8} (4s-3). \quad (\text{A.54})$$

For large values of $-\zeta$, the asymptotic expansion

$$z(\zeta) \sim \frac{\pi}{2} + \frac{2}{3} (-\zeta)^{3/2} + \mathcal{O}(|\zeta|^{-2/3}), \quad (\text{A.55})$$

is valid. Using only the first term in each of the expansions (A.48), (A.49), (A.53), and (A.54), the approximation (A.55) leads to the McMahon relations (A.45). Because of

$$\left. \begin{aligned} |\rho_1| &\lesssim 0.014, & |\rho_2| &\lesssim 0.0012 \\ |q_1| &\lesssim 0.15, & |q_2| &\lesssim 0.008. \end{aligned} \right\} \quad (\text{A.56})$$

(A.48) and (A.49) are excellent approximations. The first term $n z$ in (A.48) alone gives four-figure accuracy at $n = 4$.

B. The calculation procedure

(i) $(-\zeta) \leq 7.4$ i.e. $j_{n,s} \lesssim 15n$ or $s \lesssim 5n$: We use the first two terms of the expansions (A.48) and (A.49):

1. Input: 6 figures of Olver's table for $z(-\zeta)$ with $(-\zeta) = 0.0(0.1)7.5$, and 3 figures of $\rho_1(-\zeta)$ and $q_1(-\zeta)$.
2. Computation of the a_s, a'_s for $s \leq 35$ with an accuracy better than 0.00005.
3. Computation of $(-\zeta)_{n,s}$.
4. Computation of z from the $z(-\zeta)$ table with the help of improved linear interpolation.
5. Computation of $j_{n,s} = n z + \rho_1/n$ and $j'_{n,s} = n z + q_1/n$.

(ii) $(-\zeta) > 7.4$ i.e. $j_{n,s} \gtrsim 15n$ or $s \gtrsim 5n$: We use the improved McMahon relations [A18]

$$j_{n,s} = \frac{\pi}{4} (2n + 4s - 1) - \frac{4n^2 - 1}{2\pi(2n + 4s - 1)}, \quad (\text{A.57})$$

$$j'_{n,s} = \frac{\pi}{4} (2n + 4s - 3) - \frac{4n^2 + 3}{2\pi(2n + 4s - 3)}. \quad (\text{A.58})$$

The accuracy obtained is better than 0.0005.

(iii) $j'_{n,s=1}$: As (A.49) is too weak, the special expansion

$$j''_{n,1} = n + 0.8086165 n^{1/3} + 0.072490 n^{-1/3} - 0.05097 n^{-1}, \quad (\text{A.59})$$

is used, which yields a 0.0005 accuracy.

(iv) Small n and s : The tabulated Bessel zeros [A18] are used for $j_{0,1}$ and $j_{n \leq 4, s \leq 4}$.

C. Discussion of the accuracy

The above procedures lead to an accuracy of 0.001 for most of the zeros below 100. Only a few values have inaccuracies as large as 0.005. This is checked by

(i) comparison with the neglected third terms of Olver's expansions; (ii) comparison with the tabulated zeros for $n \leq 20$, $s \leq 50$; (iii) comparison with the calculation based on first terms only. Here, the errors are below 0.02. The second term leads to one further significant figure.

The average error relevant for the eigenvalue density is of course lower, as plus as well as minus deviations occur. It is supposed to be not larger than 0.001. This leads to the relative error

$$\left| \frac{\Delta D}{D} \right| \lesssim 0.003 \frac{\phi}{X}, \quad (A.60)$$

for the mode density $D(X)$, where $X = 2\pi R/\lambda$ and $\phi = 2R/L$. Thus, the relative error of the second order correction of the mode density is estimated by

$$\left| \frac{\Delta D_2}{D_2} \right| \lesssim 0.004 \left(\frac{\phi}{\phi + 1} \right) X. \quad (A.61)$$

This means less than 10% error for the coefficient of the second order correction in the case $\phi = 1$ and $X = 50$. Deviations of this order of magnitude were actually observed when X - and W -results (see Section 6.B) were compared with the respective first and second order corrections. We observe that, for $X \gg 100$, the above computation procedures are not sufficient for yielding the second order correction of the mode density, because the relative error increases with X according to (A.61).

Note added in proof

Recently we obtained asymptotic expansions of the averaged mode density for cavities with the shape of a prism with arbitrary cross section [157]. The mode densities of the pill-box cavity and the sectoral cavities with arbitrary sectoral angle Φ are included. For finite frequencies these expansions provide analytical formulae for the refined mode density. Within the accuracy of the numerical calculation all corresponding computer results (5.17/18), (6.11) and (6.15) *agree* with the analytical expressions. E.g. for the circular cylinder the precise second order coefficient reads $4/3 L + \pi R$, which is compatible with (6.11). On the other hand the computer results assert that asymptotic expansions for $\nu V^{1/3} \rightarrow \infty$ are valid for the far-infrared and submillimeter-wave frequency range. As far as the L dependence of the second-order coefficient is concerned, the analytical expressions are more complicated than conjectured in chapter 8. However, the R -dependent terms in (6.11) and (6.15) as well as the conjectures (5.19) and (5.20) are exact. A comparison of analytical and computational procedures in the field of mode densities is reported in a forthcoming paper [158].

Acknowledgements

The authors wish to thank Prof. Dr. R. Jost and PD Dr. H. R. Schwarz, ETH Zürich; Prof. Dr. J. Meixner, TH Aachen; Dr. E. Hilf, University of Würzburg; Dr. T. Nonnenmacher, TH Karlsruhe for their interest and many helpful discussions; as well as U. Weisner, ETH Zürich, and R. Muri, University of Geneva, for support of developing the computer programs.

This study was sponsored by the Schweizerischer Nationalfonds.

REFERENCES

- [1] D. L. STIERWALT, *Appl. Opt.* **5**, 1911 (1966).
- [2] H. E. RAST, H. H. CASPERS and S. A. MILLER, *Phys. Rev.* **169**, 705 (1968).
- [3] J. E. MOOIJ, W. B. VAN DE BUNT and J. E. SCHRIJVERS, *Phys. Lett.* **28 A**, 573 (1969).
- [4] K. HISANO, Y. OKAMOTO and O. MATUMURA, *J. Phys. Soc. Japan* **28**, 425 (1970).
- [5] R. KÄLIN, H. P. BALTES and F. K. KNEUBÜHL, *Solid St. Comms.* **8**, 1495 (1970).
- [6] F. K. KNEUBÜHL, H. P. BALTES and R. KÄLIN, review, in preparation.
- [7] R. PAPOULAR, *J. Phys.* **23**, 185 A (1962).
- [8] R. CANO and M. MATTIOLI, *Infrared Phys.* **7**, 25 (1967).
- [9] J. CHAPELLE and F. CABANNES, *J. Quant. Spectry. Radiat. Transf.* **9**, 889 (1969).
- [10] K. SHIVANANDAN, J. R. HOUCK and M. O. HARWITT, *Phys. Rev. Lett.* **21**, 1460 (1968).
- [11] D. P. McNUTT, K. SHIVANANDAN and P. D. FELDMANN, *Appl. Opt.* **8**, 2199 (1969).
- [12] D. MUELNER and R. WEISS, *Phys. Rev. Lett.* **24**, 742 (1970).
- [13] W. M. PARK, D. G. VICKERS and P. E. CLEGG, *Astron. and Astrophys.* **5**, 325 (1970).
- [14] F. J. LOW, *Astrophys. J.* **159**, L 173 (1970).
- [15] H. H. AMMANN and F. J. LOW, *Astrophys. J.* **159**, L 159 (1970).
- [16] P. STETTLER, F. K. KNEUBÜHL and E. A. MÜLLER, *Helv. phys. Acta* **42**, 630 (1969).
- [17] R. W. NOYES, *Phil. Trans. Roy. Soc.* **264 A**, 205 (1969).
- [18] A. G. KISLJAKOV, *Adv. phys. Sci.* **101**, 607 (1970) and *Sov. Phys. Uspekhi* **13**, 495 (1971).
- [19] W. L. EISENMANN, R. L. BATES and J. D. MERRIAM, *J. Opt. Soc. Am.* **53**, 729 (1963).
- [20] A. A. BUZNIKOV and B. P. KOZYREV, *J. Engng. Phys.* **9**, 53 (1965).
- [21] B. G. COLLINS, *J. Phys. E* **1**, 62 (1968).
- [22] J. M. KENDALL, Sr., Jet Propulsion Laboratory Technical Report 32-1263, May 15 (1968).
- [23] J. M. KENDALL, Sr. and C. M. BERDAHL, *Appl. Opt.* **9**, 1082 (1970).
- [24] W. J. BURROUGHS and J. E. HARRIES, *Nature* **227**, 824 (1970).
- [25] E. R. KREINS and L. J. ALLISON, *Appl. Opt.* **9**, 681 (1970).
- [26] A. S. GURVICH and V. N. YUFEREV, *Fizika Atmosfery i Okeana* **6**, 523 (1970).
- [27] A. A. PENZIAS, *IEEE Trans. MTT* **16**, 608 (1968).
- [28] C. T. STELZRIED, *IEEE Trans. MTT* **16**, 646 (1968).
- [29] P. I. SOMLO and D. L. HOLLOWAY, *IEEE Trans. MTT* **16**, 664 (1968).
- [30] T. MUKAIHATA, *IEEE Trans. MTT* **16**, 699 (1968).
- [31] C. L. TREMBATH, D. F. WAIT, G. F. EUGEN and W. J. FOOTE, *IEEE Trans. MTT* **16**, 709 (1968).
- [32] P. R. JORDAN, *Reb. Sci. Instr.* **41**, 1649 (1970).
- [33] M. PLANCK, *The Theory of Heat and Radiation* (Dover Pub., New York 1959), see p. 184.
- [34] W. WIEN and O. LUMMER, *Ann. Phys.* **292**, 451 (1895).
- [35] C. S. WILLIAMS, *J. Opt. Soc. Am.* **51**, 464 (1961), a review of earlier works.
- [36] E. M. SPARROW, L. U. ALBERS and E. R. G. ECKERT, *J. Heat Transf.* **84**, 73 (1962).
- [37] E. M. SPARROW and V. K. JONSSON, *J. Heat Transf.* **84**, 188 (1962).
- [38] E. M. SPARROW and V. K. JONSSON, *J. Opt. Soc. Am.* **53**, 816 (1963).
- [39] S. C. JAIN, *Ind. J. pure appl. Phys.* **1**, 7 (1963).
- [40] S. H. LIN and E. M. SPARROW, *J. Heat Transf.* **87**, 299 (1965).
- [41] P. CAMPANARO and T. RICOLFI, *Appl. Opt.* **5**, 1271 (1966).
- [42] V. M. MELENT'EV, *High Temp.* **6**, 295 (1966).
- [43] F. J. KELLY, *Appl. Opt.* **5**, 925 (1966).

- [44] T. J. QUINN, Brit. J. appl. Phys. 18, 1105 (1967), includes review.
- [45] P. CAMPANRRO, T. RICOLFI, J. Opt. Soc. Am. 57, 48 (1967).
- [46] YU. G. ZHULEV and V. A. KOSARENKO, High Temp. 5, 161 (1967).
- [47] M. L. FECTEAU, Appl. Opt. 7, 1363 (1968).
- [48] V. M. MELENT'EV, High Temp. 6, 851 (1968).
- [49] F. E. NICODEMUS, Appl. Opt. 7, 1359 (1968).
- [50] S. P. RUSSIN, High Temp. 6, 529 (1968).
- [51] G. K. KHOPOLOV, High Temp. 7, 226 (1969).
- [52] J. O. SACADURA and L. SICARD, C. r. Acad. Sci. [Paris] B 271, 191 (1970).
- [53] E. M. SPARROW and R. P. HEINISCH, Appl. Opt. 9, 2569 (1970).
- [54] J. C. DE VOS, Physica 20, 669 (1954).
- [55] C. S. WILLIAMS, J. Opt. Soc. Am. 59, 249 (1969).
- [56] B. A. PEAVY, J. Res. Natl. Bur. Stand. 70 C, 139 (1966).
- [57] G. J. BIRGER, Measurem. Techn. 7, 909 (1966).
- [58] V. B. FEDOROV and V. S. EGOROV, High Temp. 6, 473 (1968).
- [59] E. M. SPARROW and T. M. KUZAY, J. Heat Transf. 91, 285 (1969).
- [60] G. BAUER and K. BISCHOF, Optik 31, 507 (1970).
- [61] G. BAUER, Optik 18, 603 (1961).
- [62] F. J. KELLY and D. G. MOORE, Appl. Opt. 4, 31 (1965).
- [63] G. BAUER, Optik 28, 177 (1968/69).
- [64] R. P. HEINISCH and R. N. SCHMIDT, Appl. Opt. 9, 1920 (1970).
- [65] T. J. QUINN, J. Sci. Instr. 44, 221 (1967).
- [66] W. FISCHER and D. LABS, Z. Instrum.-Kunde 75, 226 (1967).
- [67] J. A. HALL, J. Sci. Instr. 44, 257 (1967).
- [68] H. Y. YAMANADA, Appl. Opt. 6, 357 (1967).
- [69] E. H. GEYER and W. PIEPER, Feingeräte-Techn. 16, 153 (1967).
- [70] T. J. QUINN and M. C. FORD, Proc. Roy. Soc. A 312, 31 (1969).
- [71] G. FRIEDE and R. MANNKOPF, Z. angew. Phys. 28, 357 (1970).
- [72] R. W. REYNOLDS, Electro-Technology 71, 1 (1963).
- [73] J. C. RICHMOND, W. N. HARRISON and F. J. SHORTEN, *Measurements of Thermal Radiation Properties of Solids*, NASA SP-31, 403 (1963); J. C. RICHMOND, ed.
- [74] H. E. CLARK and D. G. MOORE, *Symposium on the Thermal Radiation of Solids*, NASA SP-55, 241 (1965), S. KATZOFF, ed.
- [75] F. E. BLISS, S. DAVID and B. STEIN, Appl. Opt. 9, 2033 (1970).
- [76] E. DUVERNOY, Messtechnik 5, 129 (1969), review.
- [77] M. W. P. CANN, Appl. Opt. 8, 1645 (1969), review.
- [78] R. PAPOULAR, Infrared Phys. 4, 137 (1964).
- [79] SH. A. BEZVERKHNI, L. P. BOGDANOVA and M. A. BRAMSON, Instr. Exp. Techn. 5, 405 (1966).
- [80] A. J. LICHTENBERG and S. SESNIK, J. Opt. Soc. Am. 56, 75 (1966).
- [81] O. K. FILIPPOV and E. V. UKHANOV, Instr. Exp. Techn. 6, 1399 (1967).
- [82] A. R. KAROLI, J. R. HICKEY and R. E. NELSON, Appl. Opt. 6, 1183 (1967).
- [83] A. LA ROCCA and G. ZISSIS, Rev. Sci. Instr. 30, 200 (1959).
- [84] H. RUBENS and F. KURLBAUM, Ann. Phys. 4, 649 (1901).
- [85] H. RUBENS and G. MICHEL, Phys. Z. 22, 569 (1921).
- [86] W. R. BLEVIN, Metrologia 6, 39 (1970).
- [87] C. J. BOUKAMP, Diss. 1941, repr. in IEEE Trans. AP-18, 152 (1970).
- [88] C. J. BOUKAMP, Rept. Progr. Phys. 17, 35 (1954), review.
- [89] J. MEIXNER and W. ANDREJEWSKI, Ann. Phys. 7, 157 (1950).
- [90] W. ANDREJEWSKI, Z. angew. Phys. 5, 178 (1953).
- [91] P. FACQ, C. r. Acad. Sc. [Paris] B 269, 171 (1969).
- [92] H. P. BALTES and F. K. KNEUBÜHL, Helv. phys. Acta 42, 628 (1969).
- [93] H. P. BALTES, R. MURI and F. K. KNEUBÜHL, Microwave Res. Inst. Symposia Series 20, 667 (1970), J. Fox ed., Press of the Polytechnic Institute of Brooklyn, N. Y., USA.
- [94] L. D. LANDAU and E. M. LIFSHITZ, *Statistical Physics* (Pergamon Press, London 1959).
- [95] A. EINSTEIN, Phys. Z. 10, 185 (1909).
- [96] A. EINSTEIN, in: *La théorie du rayonnement et les quanta*, edited by P. LANGEVIN and M. DE BROGLIE, 1912, p. 427 (Congrès Solvay 1912).

- [97] W. PAULI, in: *A. Einstein, Philosopher-Scientist*, edited by P. A. SCHILPP, 1949, p. 149–160.
- [98] R. FÜRTH, *Z. Phys.* **50**, 310 (1928).
- [99] R. C. BOURRET, *Nuovo Cim.* **18**, 347 (1960).
- [100] Y. KANO and E. WOLF, *Proc. Phys. Soc.* **80**, 1273 (1962).
- [101] C. L. MEHTA and E. WOLF, *Phys. Rev.* **134**, A 1143 (1964).
- [102] L. MANDEL and E. WOLF, *Rev. mod. Phys.* **37**, 231 (1965), review.
- [103] R. FÜRTH, *Proc. Roy. Soc. Edinburgh*, *A* **67**, 269 (1967).
- [104] A. KUJAWSKI, *Acta phys. pol.* **34**, 957 (1968).
- [105] A. EINSTEIN, *Phys. Z.* **18**, 121 (1917).
- [106] W. E. LAMB, Jr., *Rep. Progr. Phys.* **14**, 19 (1951), review.
- [107] W. PAULI, *Theorie der Schwarzen Strahlung*, in: *Collected Scientific Papers*, vol. 1, edited by R. KRONIG and V. F. WEISSKOPF, 1964, p. 565–653.
- [108] T. H. BOYER, *Phys. Rev.* **182**, 1374 (1969).
- [109] S. R. BARONE, Air Force Cambridge Res. Lab. Report AFCRL-65-228 (1965) and Proc. XX PIB Symposium on Submillimeterwaves, New York, March/April 1970.
- [110] K. H. DREXHAGE, *Sci. Am.* **22/3**, 108 (1970).
- [111] J. C. SLATER, *Microwave Electronics* (van Nostrand Comp. Inc., Princeton, N. J. 1954).
- [112] F. E. BORGNIS and C. H. PAPAS, *Electromagnetic Waveguides and Resonators*, in *Encyclopedia of Phys.* **16**, 285 (1958).
- [113] K. PÖSCHL, *Mathematische Methoden der Hochfrequenztechnik* (Springer Verlag, Berlin 1956).
- [114] W. K. F. PANOFSKY and M. PHILLIPS, *Classical Electricity and Magnetism* (Addison-Wesley Pub. Comp. Inc., Reading, Mass. 1955), 2nd ed. 1962.
- [115] C. MÜLLER and H. NIEMEYER, *Arch. ration. mech. Anal.* **7**, 305 (1961).
- [116] D. S. JONES, *The Theory of Electromagnetism* (MacMillan Book Comp., 1964), Ch. IV.
- [117] F. BORGNIS, *Ann. Phys. Lpz.* **35**, 359 (1939).
- [118] A. NISBET, *Proc. Roy. Soc.* **231 A**, 250 (1955).
- [119] G. TYRAS, *Radiation and Propagation of Electromagnetic Waves* (Academic Press, New York 1969).
- [120] A. WEXLER, *IEEE Trans. MTT* **17**, 416 (1969), review.
- [121] D. T. THOMAS, *IEEE Trans. MTT* **17**, 447 (1969).
- [122] L. GÅRDING, *Math. Scand.* **1**, 237 (1953).
- [123] B. V. FEDOSOV, *Dokl. Akad. Nauk SSSR, Ser. Mat. Fiz.* **157**, 536 (1964) and *Soviet Math. Dokl.* **5**, 988 (1964).
- [124] R. BALIAN and C. BLOCH, *Ann. Phys.* **60**, 401 (1970).
- [125] R. BALIAN and C. BLOCH, *Ann. Phys.* **64**, 271 (1971).
- [126] F. H. BROWNELL, *J. Math. Mech.* **6**, 119 (1957).
- [127] K. M. CASE and S. C. CHIU, *Phys. Rev. A* **1**, 1170 (1970).
- [128] F. POCKELS, *Über die partielle Differentialgleichung $\Delta u + k^2 u = 0$ und deren Auftreten in der mathematischen Physik* (B. G. Teubner, Leipzig 1891).
- [129] J. H. JEANS, *Phil. Mag.* **10**, 91 (1905).
- [130] Lord RAYLEIGH (= J. W. STRUTT), *Nature* **72**, 54, 243 (1905).
- [131] H. WEYL, *Math. Ann.* **71**, 441 (1911).
- [132] H. WEYL, *J. reine u. angew. Math.* **141**, 163 (1912).
- [133] D. HILBERT, *Gesammelte Abhandlungen*, Vol. III, 2nd ed. (Springer Verlag, Berlin 1970).
- [134] R. COURANT and D. HILGERT, *Methods of Mathematical Physics*, Vol. I, Ch. V, (Interscience Pub. Inc., New York 1953).
- [135] M. KAC, *Am. Math. Monthly* **23**, 4, 1 (1966).
- [136] M. PLANCK (editor), *Abhandlungen über Emission und Absorption von G. Kirchhoff*, Ostwalds Klassiker, exakt. Wiss. **100**, comment no. 6 on p. 38 (Verlag W. Engelmann, Leipzig 1898).
- [137] H. WEYL, *J. reine u. angew. Math.* **143**, 177 (1913).
- [138] T. CARLEMAN, *Huitième Congr. Math. Scand. à Stockholm*, 1934, p. 34, and *Collected Works*, Malmö 1960, p. 471.
- [139] T. CARLEMAN, *Ber. Sächs. Akad. d. Wissensch. Leipzig*, **88**, 119 (1936) and *Collected Works*, Malmö, 1960, p. 483.
- [140] I. KARAMATA, *J. reine u. angew. Math.* **164**, 27 (1931).
- [141] H. NIEMEYER, *Arch. rational. mech. Anal.* **7**, 412 (1961).
- [142] C. CLARK, *SIAM Rev.* **9**, 627 (1967).

- [143] Å. PLEIJEL, Tolfte Skandinaviska Matematiker Kongressen, Lund 1954, p. 222 and *Ark. Mat.* 2, 553 (1954).
- [144] E. HILF, *Z. Naturforsch.* 25 A, 1190 (1970).
- [145] K. STEWARTSON and R. T. WAECHTER, *Proc. Camb. Phil. Soc.* 69, 353 (1971).
- [146] D. L. HILL and J. A. WHEELER, *Phys. Rev.* 89, 1102 (1953), particularly p. 1124.
- [147] E. HILF and G. SÜSSMANN, *Phys. Lett.* 21, 654 (1966).
- [148] E. HILF, Diplomarbeit, Universität Frankfurt, 1963.
- [149] E. HILF, Dissertation, Universität Frankfurt, 1967.
- [150] H. P. BALTES, *Helv. phys. Acta* 44, 589 (1971) and to be published.
- [151] N. WIENER, *The Fourier integral and certain of its applications* (Cambridge 1933).
- [152] W. SCHWARZ, *Der Primzahlsatz*, Überblicke Mathematik 1, 35 (1968); BI-Hochschultaschenbuch 161/161a.
- [153] W. R. BLEVIN and W. J. BROWN, *Metrologia* 7, 15 (1971).
- [154] B. W. JOLLEY, *Summation of Series* (Dover Pub., New York 1961), No. 124, p. 22.
- [155] E. T. WHITTAKER and G. N. WATSON, *A Course of Modern Analysis* (Cambridge 1969), 4th ed., p. 265.
- [156] H. P. BALTES, submitted to *Int. J. of Appl. Phys.*
- [157] H. P. BALTES, *Phys. Letters* 38A, 523 (1972) and to be published in *Phys. Rev. A3* (1972).
- [158] H. P. BALTES and E. HILF, to be published in *Computer Phys. Comms.*

REFERENCES USED IN APPENDIX

- [A1] G. H. HARDY and E. M. WRIGHT, *An Introduction to the Theory of numbers* (Clarendon Press, Oxford 1959), 4th ed.
- [A2] C. F. GAUSS, *Disquisitiones Arithmeticae* (Leipzig 1801), reprinted in vol. I of Gauss's Werke, p. 272.
- [A3] W. SIERPIŃSKI, *Prace mat.-fix.* [Warsaw] 17, 77 (1906).
- [A4] E. LANDAU, *Nachr. d. Ges. d. Wiss. [Göttingen]* 1915, p. 148.
- [A5] G. H. HARDY, *Quart. J. Math.* 46, 263 (1915).
- [A6] J. G. VAN DER CORPUT, *Math. Z.* 17, 250 (1923).
- [A7] J. E. LITTLEWOOD and A. WALFISZ, *Proc. Roy. Soc. A* 106, 478 (1924).
- [A8] L. W. NIELAND, *Math. Ann.* 98, 717 (1928).
- [A9] E. C. TITCHMARSH, *Proc. London Math. Soc.* (2) 38, 96, 555 (1935).
- [A10] I. VINOGRADOV, *Bull. Acad. Sci. URSS* 7, 313 (1932), refereed in: *Zentralbl. f. Math.* 5, 247 (1933).
- [A11] WEN-LIN YIN, *Sci. Sinica* 11, 10 (1962).
- [A12] G. EISENSTEIN, *J. reine u. angew. Math.* 35, 368 (1847).
- [A13] E. LANDAU, *Nachr. d. Ges. d. Wiss. [Göttingen]*, p. 693, 764 (1912).
- [A14] W. SIERPIŃSKI, *Spraw. Towarz. Nauk* (Proc. Sci. Soc. [Warsaw]) 2, 117 (1909).
- [A15] E. LANDAU, *Arch. Math. Phys.* (3) 13, 305 (1908).
- [A16] E. HILF and H. P. BALTES, to be published.
- [A17] M. ABRAMOWITZ and I. A. STEGUN (ed.), *Handbook of Mathematical Functions with Formulas, Graphs and Mathematical Tables*, NBS AMS (1964).
- [A18] F. W. J. OLVER (ed.), *Roy. Soc. Math. Tables*, vol. 7: *Bessel Functions, Part III: Zeros and Associated Values* (Cambridge 1960).
- [A19] F. W. J. OLVER, *Phil. Trans. Roy. Soc. [London]* A 247, 38 (1954).
- [A20] F. W. J. OLVER, *Phil. Trans. Roy. Soc. [London]* A 247, 328 (1954).
- [A21] B. DÖRING, *Nullstellen von Zylinderfunktionen und verwandten Funktionen – Verfahren zur Bestimmung und Fehlerabschätzung* (Dissertation, Techn. Hochschule Darmstadt 1964).
- [A22] J. McMAHON, *Ann. Math.* 9, 23 (1894/95).